On the Adiabatic Piston Problem

Simulations and H-theorem for a Fokker-Planck type equation

by

Blas Ángel Loyens

to obtain the degree of Bachelor of Science
at the Delft University of Technology,

Student number:	5623707	
Project duration:	March 5, 2024 – June 21, 2024	
Thesis committee:	Dr. H. Yoldaş,	TU Delft, supervisor
	Dr. ir. D. Lathouwers,	TU Delft, supervisor
	Dr. B. Janssens,	TU Delft
	Dr. M. Goorden,	TU Delft

TU Delft

Abstract

In this project, Boltzmann's $\mathscr{H}$-theorem is studied and applied to prove a general convergence to equilibrium for the adiabatic piston paradox, governed by a specially-derived kinetic Fokker-Planck equation. We review general results in kinetic theory on the Boltzmann collision operator, and rates of convergence to equilibrium. Furthermore, we turn our attention to simulations of the piston paradox, and apply the algorithm of Sigureirsson et al. for particle-particle collision dynamics to the piston setting, determining empirically the optimal parameters.

Contents

1 Introduction

The adiabatic piston paradox has been a thermodynamical peculiarity since it was first introduced around the 1960s in [5]. A seemingly innocent problem, it describes a isolated cylinder of gas split into two volumes by a friction-less, heavy, adiabatic piston. The core of the paradox lies in taking the correct thermodynamic limits and applying the correct principles, to find the action of the piston as the pressures on both sides of the piston become equal. To this end, elementary thermodynamics could not accurately describe the final equilibirum state (of equal temperatures), requiring the use of non-equilibrium thermodynamics [26] to do so. One approach is to look at the problem from the micro- and mesoscopic point of view. That is to say, to account for each individual gas molecule (microscopic scale) and its dynamics through classical mechanics, and derive general trends by describing the probability distributions governing the gas molecules (mesoscopic scale).

This approach lies at the heart of kinetic theory, bridging the gap between the microscopic description and bulk properties of materials and gases. For gases, this was predominantly formalized through Boltzmann's work [3] in the 1870s, though the ideas existed in some form already in the times of Clausius [24]. At the time, the theory was controversial, as even the existence of atoms was not yet fully agreed upon. In the many years since, we find it now accurately describes a whole range of physics, from aeronautics at high altitudes, to plasma physics. As long as the gas is dilute enough it can often be well described through the kinetic framework introduced by Boltzmann [30].

With his treatise work, however, Boltzmann also showed from some assumptions, in particular on the micro-reversibility of the system and the molecular chaos assumption, that a macroscopic property $\mathscr{H}$ is strictly non-decreasing in time, the result being known as the (Boltzmann) $\mathscr{H}$-theorem. This property was namely entropy (up to a sign), and can be considered a manifestation of the second law of thermodynamics. This also formalized the beginnings of the study of convergence to equilibrium in kinetic models. Since then, results from varying fields, in particular information theory [16, 17] have been used to prove both convergence and the rate of convergence to equilibrium for a growing variety of kinetic equations [1, 22].

This convergence to equilibrium is of particular interest for the piston paradox. Models have been made in simplified versions of the paradox, where certain scaling limits are taken to retrieve different descriptions [6, 21]. Under these limits, and with the help of some assumptions, results on the (in)stability of the piston paradox help shed more light on the long-term dynamics of the system [4].

However, as with a lot of results in kinetic theory, many arguments are difficult to prove from a rigorous mathematical perspective. With the increasing processing capabilities of modern computers, large-scale models have become feasible and indeed actively sought after, to confirm assumptions or numerically determine new results [6, 19, 21]. Results on equilibrium convergence, for example, can be tested empirically by running simulations for long time frames [4, 9, 10]. In order to maximize the available processing power, more efficient algorithms are employed [29], enabling more results to be obtained in a shorter time-span.

We will mention that when it comes to the topics of kinetic theory, the treatise works of Villani [30] and Cercigani [7] are invaluable. Not only do they cover a broad number of topics within the field, but with plenty

of detail, referring as necessary to further reading. This thesis is in large part a combination of the results of [30], [29] and [9]. The aim of this thesis is to introduce the framework of kinetic theory in the context of the adiabatic piston paradox, allowing us to eventually prove an equivalence to equilibrium using a specially derived kinetic Fokker-Planck equation for the paradox. Furthermore, we discuss simulation techniques and adapt them in the piston context, allowing for future work to validate the assumptions made during the derivation of the Fokker-Planck equation.

In Chapter 2, we cover the physics behind the paradox, and the main assumptions and results of kinetic theory, deriving some simple results to be used in future chapters.

In Chapter 3, we discuss in depth the paradox from a simulation perspective, recapping and reproducing some results, and implementing and optimizing a new algorithm.

In Chapter 4, we state and prove general convergence to equilibrium results, and where possible the rate of convergence too. In doing so, we provide an insight of how such results are proven in the general case.

In Chapter 5, we derive a Fokker-Planck equation for the piston in the near-equilibrium paradox setting in a torus.

And lastly a conclusion and discussion on future work in Chapter 6.

2

Adiabatic piston paradox & a brief introduction to kinetic theory

In this chapter, we will describe more thoroughly the details of the adiabatic piston paradox, and some of the mathematical language that will be recurring throughout this thesis.

2.1. The Paradox

We consider an isolated cylinder, split into two equal volumes, V_1, V_2, by a piston. This piston can move freely along the cylinder without friction, and does not permit the transfer of particles nor heat between the two compartments. The prohibition of heat transfer is why the piston is called *adiabatic*. We also set the pressures P_1, P_2 to be equal on both sides of the piston, but the temperatures are different: $T_1 \neq T_2$. The paradox is then as follows: **Does the piston move?**

2.1.1. Why the piston shouldn't move

Heuristically, one may argue that the piston can only move due to mechanical work in the system. Since work done by a system is given by $dW = PdV$, and the pressures on both sides are equal, we would expect there to be no work done, and consequently that the piston *cannot* move. For a formal description of this argument, we follow Callen [5], who introduced the paradox in the first place. We note first that this whole setup is quasi-static, so we can freely work with most of the thermodynamical machinery. The first law of thermodynamics, following the convention of Clausius, can be written as $\Delta U = Q - W$, where ΔU denotes the change in internal energy of a system, Q the heat transferred *to* the system, and W the work done *by* the system (hence the minus sign). This is in effect a conservation of energy equation, which can be re-written for quasi-static processes in terms of each variable's differentials, namely $dU = dQ - dW$. We have established that there is no heat transfer, so $dQ = 0$. Moreover, we know $dW_{1,2} = P_{1,2}dV_{1,2}$ so we have an expression for the change in internal energies. The system is wholly isolated, so the total internal energy must remain constant. This gives rise to:

$$dU = dU_1 + dU_2 = 0 \implies P_1 dV_1 + P_2 dV_2 = 0 \tag{2.1}$$

We also have that the total volume $V = V_1 + V_2$ is fixed, giving us $dV_1 = -dV_2$. It is evident that equation (2.1) holds only if $P_1 = P_2$, which is the case. We consider now entropy, $S(U, V)$. For both sides we have:

$$dS_{1,2} = \frac{dU_{1,2}}{T_{1,2}} + \left(\frac{P}{T}dV\right)_{1,2}$$

However, from our conclusion that $dU_{1,2} = -P_{1,2}dV_{1,2}$ it's clear that $dS_{1,2} = 0$ and so the total entropy change $dS = dS_1 + dS_2 = 0$ is constant. The entropy maximum principle, often referred to as the second-law, tells us $dS = 0$ only holds at equilibrium, and so the piston *will not move*.

2.1.2. Why the piston should move

However, if the problem was this open-and-shut, it wouldn't be a paradox. There is a second, more subtle argument that argues the converse, that the piston *does* move. It involves the second law of thermodynamics,

and very careful algebraic manipulations. There is a heuristic argument too, outlined in Feynman's famous lectures [14, Ch. 39-4]. Although the pressures are equal, they describe only the average kinetic energy *density* of the particles. The temperatures themselves describe the average kinetic energy, and so the warmer side will hit the piston wall with (on average) higher velocities. This would lead to the piston drifting towards the colder side, where there would be a higher particle density and so more collisions, which would pick up the excess speed of the piston. This transfer of kinetic energy would continue until the kinetic energies are equal, giving us $T_1 = T_2$.

Making this argument precise is more tedious. The principal disagreement with the former argument is that $dU_{1,2} \neq -P_{1,2}dV_{1,2}$, and thus that the whole application of the entropy maximum principle is wholly inappropriate [18]. Indeed, if this were the case, then the total energy would not be constant in the general case. We would have the change in total energy

$$dU = dU_1 + dU_2 = -P_1 dV_1 + P_2 dV_2 = -(P_1 - P_2)dV_1 \neq 0$$

be in general non-zero for $P_1 \neq P_2$. We would then be maximizing entropy for a system that is potentially losing or gaining energy, and if we cannot quantify such gains then applying the second law of thermodynamics would be nonsensical. As [18] describes, the lost energy must be accounted for in some way or other, most naturally through 'heat' $dQ = (P_1 - P_2)dV_1$. The paper goes through in detail of different approaches to then derive the conclusion that equilibrium is only found at thermal equilibrium (that is to say, $P_1 = P_2$ is necessary, but not sufficient). If we accept the general formulation of internal energy to be $dU = TdS - PdV$ (even though the former term is often associated with 'heat'), then we can assure total energy remains constant. We now get:

$$dU = dU_1 + dU_2 = 0 \implies T_1 dS_1 - P_1 dV_1 = P_2 dV_2 - T_2 dS_2$$

Assuming $P_1 = P_2$, and applying once again $dV_2 = -dV_1$, this gives us the relation

$$T_1 dS_1 = -T_2 dS_2 \tag{2.2}$$

By the second law of thermodynamics, we have $dS = dS_1 + dS_2 \geq 0$, and multiplying throughout by T_1 gives $T_1 dS_1 + T_1 dS_2 \geq 0$. Substituting in (2.2) gives us:

$$(T_1 - T_2)dS_2 \geq 0 \tag{2.3}$$

Equality holds when $T_1 = T_2$, though care must be taken to not discount $dS_2 = 0$. In particular, for the case where $T_1 > T_2$, we see that $dS_2 \geq 0$, so the entropy of the colder subsystem increases over time. Returning to the paradox, since we start with $T_1 \neq T_2$, it is clear that the entropy of the system is not maximal, and so the system is not in an equilibrium state, so the piston *will move* to accommodate it.

2.1.3. General remarks

There are many discussions and subtleties in the arguments presented above. Some argue that the whole paradox is not a feasible setup as no rigid body like the piston in our setup can act as a perfect insulator. By virtue of the fact that it allows for the transfer of kinetic energy between the two compartments, it must therefore allow the transfer of heat. Then there is also the question of how quickly the system converges to first mechanical equilibrium $P_1 = P_2$ and then thermal equilibrium, $T_1 = T_2$. The latter is expected to occur on a timescale much larger than the former. We will be taking a microscopic approach to the problem, accounting for each gas particle and seeing how its velocity develops over time. For this, we need to describe the mathematical language in this setting.

2.2. Mathematical description of kinetic theory

In this section, we will follow the treatise work of Villani [30].

2.2.1. Modelling framework

The objective of kinetic theory, is to model the evolution of gas by a distribution function in the particle phase space. In the simplest case, for a classical gas made up of only one type of particle, we find that the corresponding kinetic model is the function:

$$f(t, \vec{x}, \vec{v}) : [0, T] \times \Omega \times \mathbb{R}^d \to [0, \infty)$$

Where $\Omega \subset \mathbb{R}^d$ is the spatial domain of the gas (that may or may not be bounded) and d the dimension of the space (typically 3). For any time t, the quantity $f(t,\vec{x},\vec{v})d\vec{x}d\vec{v}$ gives the density of particles in the volume element $d\vec{x}d\vec{v}$ centered on $(\vec{x},\vec{v})$. This interpretation means that f must act as a scaled probability measure over $(\vec{x},\vec{v})$, and since we are dealing with the case of finite number of particles, we quickly conclude that $f(t,\cdot,\cdot) \in L^1(\Omega,\mathbb{R}^d)$. From the probability density function, we can recover measurable macroscopic quantities. Indeed, we have the following:

Definition 2.2.1 (Macroscopic qualities)**.** From the density function we can define:

- ρ, the local density, by: $\rho(t,\vec{x}) := \int_{\mathbb{R}^d} f(t,\vec{x},\vec{v})\, d\vec{v}$
- $\vec{u}$, the local macroscopic velocity, by the relation: $\rho\vec{u} = \int_{\mathbb{R}^d} f(t,\vec{x},\vec{v})\vec{v}\, d\vec{v}$
- T, the local temperature, by the relation: $\rho|u|^2 + d\rho T = \int_{\mathbb{R}^d} f(t,\vec{x},\vec{v})|v|^2\, d\vec{v}$

To describe the time evolution of gas, the first commonly encountered term is the transport operator. If we completely neglect interaction between particles, then each particle travels at constant velocity and so the probability density is constant along characteristic lines $d\vec{x}/dt = \vec{v}, d\vec{v}/dt = 0$. Indeed, under these circumstances, we can compute f at any arbitrary time t simply from the initial distribution at time 0:

$$f(t,\vec{x},\vec{v}) = f(0,\vec{x}-\vec{v}t,\vec{v})$$

Functions that satisfy the above equation are weak solutions to the following **equation of free transport**:

$$\partial_t f + \vec{v}\cdot\nabla_x f = 0 \tag{2.4}$$

Where $\partial_t f$ denotes the partial time derivative of f (also often written as $\partial f/\partial t$), and ∇_x denotes the gradient operator in the $\vec{x}$ components of f, i.e. $[\partial_{x_1},\ldots,\partial_{x_d}]^T$. Whilst the transport operator, $\vec{v}\cdot\nabla_x$ crops up in many equations in kinetic theory, we will not be using it in this thesis. The principle reason for this is that all solutions of the transport equation (2.4) do not contribute to a change in functionals of the form $\int_{\Omega\times\mathbb{R}^d} A(f)\, d\vec{x}\, d\vec{v}$. More strongly, the transport operator *itself* does not contribute a change to the aforementioned functional.

Lemma 2.2.2. *In the case of $\Omega = \mathbb{R}^d$, the transport operator $\vec{v}\cdot\nabla_x$ does not contribute to the change of functionals of the form $\int_{\mathbb{R}^d\times\mathbb{R}^d} A(f)\, d\vec{x}\, d\vec{v}$. More specifically, if f satisfies the equation:*

$$\partial_t f + \vec{v}\cdot\nabla_x f = Q(f,t,\vec{x},\vec{v})$$

Where Q is some arbitrary function that may or may not depend on the listed variables, then the time evolution of the functional is decided entirely by Q:

$$\frac{d}{dt}\int_{\mathbb{R}^d\times\mathbb{R}^d} A(f)\, d\vec{x}\, d\vec{v} = \int_{\mathbb{R}^d\times\mathbb{R}^d} A'(f)Q\, d\vec{x}\, d\vec{v}$$

Proof. Ignoring any particular regularity constraints, we have that:

$$\frac{d}{dt}\int_{\mathbb{R}^d\times\mathbb{R}^d} A(f)\, d\vec{x}\, d\vec{v} = \int_{\mathbb{R}^d\times\mathbb{R}^d} A'(f)\partial_t f\, d\vec{x}\, d\vec{v} = \int_{\mathbb{R}^d\times\mathbb{R}^d} A'(f)Q\, d\vec{x}\, d\vec{v} - \int_{\mathbb{R}^d\times\mathbb{R}^d} A'(f)\vec{v}\cdot\nabla_x f\, d\vec{x}\, d\vec{v}$$

The claim is equivalent to showing that the last integral evaluates to 0. In 1D this is clear, as $\Omega = (-\infty,\infty)$. The last integral reads:

$$\int_{\mathbb{R}\times\mathbb{R}} A'(f)v\partial_x f\, dx\, dv = \int_{\mathbb{R}} v\int_{-\infty}^{\infty} A'(f)\partial_x f\, dx\, dv = \int_{\mathbb{R}} v\Big[A(f)\Big]_{-\infty}^{\infty} dv$$

But at the boundary, it is clear $f(t,-\infty,v) = f(t,\infty,v) = 0$, due to the convergence on the integral $\int_{\mathbb{R}} f\, dx$ and so the boundary term evaluates to $A(0) - A(0) = 0$. In the higher dimensional case, we would have the exact same argument, with the boundary term evaluated on the limiting disk $|\vec{x}| = r$ as $r\to\infty$ (or really any other unbounded domain that reaches infinity in all coordinates. A hypercube also works here). The integrability of f demands $\lim_{|\vec{x}|\to\infty} f(t,\vec{x},\vec{v}) = 0$. Suppose it didn't, i.e. $\lim_{|\vec{x}|\to\infty} f(t,\vec{x},\vec{v}) = C(t,v) > 0$ for some constant C possibly depending on t, v. Then there certainly is a disk r such that $\forall\vec{x}\in\mathbb{R}^d, |\vec{x}| \geq r, f(t,\vec{x},\vec{v}) \geq \frac{C}{2}$. Then:

$$\int_{\mathbb{R}^d} f\, d\vec{x} \geq \int_{|\vec{x}|\geq r} f\, d\vec{x} \geq \int_{|\vec{x}|\geq r} \frac{C}{2}\, d\vec{x} \to \infty$$

Where we note the last integral diverges to infinity. This contradicts the integrability of f, and so we conclude that f vanishes at the boundary (and so $A(f)$ is constant at the boundary). In peculiar cases where $\lim_{|\vec{x}|\to\infty} f(t,\vec{x},\vec{v})$ does not exist, then one can find a ray from the origin where $f>0$ infinitely many times, and apply a similar argument on this ray. □

We remark that the transport operator also doesn't contribute to functionals when $\Omega = \mathbb{T}^d$, the d-dimensional torus (which can be thought of, in a physical sense as a constrained space of the form $[\vec{0},\vec{1}]$, with periodic boundary conditions). In any case, the transport operator is not the only term that can influence the progression of f over time. External forces can also impact f (giving rise to linear Vlasov equation, see [30, p. 10]), but we are more interested in the impact of gas particle collisions. For this, we have the Boltzmann collision operator.

2.2.2. Boltzmann collision operator

To describe the evolution of f due to collisions, a series of assumptions must be made.

Assumption 1. Particles interact via **binary collisions**, that is to say collisions only occur between two particles, and the chances of a collision involving three or more particles is vanishingly small, which implies that the gas is dilute. Indeed, for a 3 dimensional gas of N hard spheres with radius r, this would mean:

$$Nr^3 \ll 1, \qquad Nr^2 \simeq 1 \tag{2.5}$$

Assumption 2. These collisions are **localized** in both space and time, so they are brief events that occur at a position $\vec{x}$ and time t.

Assumption 3. The collisions are **elastic**, momentum and kinetic energy are conserved in the collision process. If $\vec{v},\vec{v}_*$ are the velocities of two particles *before* colliding, and $\vec{v}',\vec{v}'_*$ the respective velocities *after* colliding, then we find these variables must satisfy:

$$\vec{v}+\vec{v}_* = \vec{v}'+\vec{v}'_* \tag{2.6}$$

$$|\vec{v}|^2+|\vec{v}_*|^2 = |\vec{v}'|^2+|\vec{v}'_*|^2 \tag{2.7}$$

Equation (2.6) is over d dimensions, and equation (2.7) is 1 equation, but together they can be used to calculate the $2d$ unknown values, v',v'_*. As a consequence, we expect to describe the solutions to the equations in terms of $d-1$ parameters. There is a convenient representation of these solutions, aptly called the σ-**representation**, where the parameter $\sigma\in\mathbb{S}^{d-1}$ lies on the $(d-1)$-dimensional unit sphere in $\mathbb{R}^d$. The representation is as follows:

$$\vec{v}' = \frac{\vec{v}+\vec{v}_*}{2} + \frac{|\vec{v}-\vec{v}_*|}{2}\sigma$$

$$\vec{v}'_* = \frac{\vec{v}+\vec{v}_*}{2} - \frac{|\vec{v}-\vec{v}_*|}{2}\sigma$$

Assumption 4. We assume the collisions to be **microreversible**. There are two interpretations of this. One is deterministic, that the microscopic dynamics are time-reversible. The other is probabilistic, that the probability that the velocities $(\vec{v},\vec{v}_*)$ are changed to $(\vec{v}',\vec{v}'_*)$ is equal to the probability that the velocities $(\vec{v}',\vec{v}'_*)$ are changed to $(\vec{v},\vec{v}_*)$

Assumption 5. Lastly, we have the Boltzmann **chaos** assumption, or more broadly, molecular chaos: the velocities of the two particles which are about to collide are uncorrelated. This assumption implies an asymmetry between past and future, as collision velocities are certainly correlated. For a deep and entertaining discussion on the physical validity of this assumption and its apparent contradiction with the microreversibility assumption, see [30, pgs. 34-37]

Under the above 5 assumptions, Boltzmann [3] was able to derive the following collision operator:

Definition 2.2.3 (Boltzmann collision operator)**.** The Boltzmann collision operator is given by:

$$Q(f,f) = \int_{R^d}\int_{\mathbb{S}^{d-1}} B(\vec{v}-\vec{v}_*,\sigma)\left(f'f'_* - ff_*\right)d\sigma\, d\vec{v}_* \tag{2.8}$$

Where we use the abbreviations $f'=f(t,\vec{x},\vec{v}'), f_*=f(t,\vec{x},\vec{v}_*), f'_*=f(t,\vec{x},\vec{v}'_*)$ and where $B(\vec{z},\sigma)$ is called the **Boltzmann collision kernel**. The function is non-negative and can be simplified further as a function of $|\vec{z}|$ and the scalar product $\hat{z}\cdot\sigma=\cos\theta$, where θ is the deviation angle (between the pre- and post- collision velocities).

Before we proceed, let us observe a few critical properties about the form of the Boltzmann collision operator. Firstly, it is quadratic in f, which follows from assumption **1**, namely the binary nature of the collisions. Moreover, the operator can be split into a *gain* and *loss* term $Q(f,f) = Q^+(f,f) - Q^-(f,f)$. The interpretation of these terms are as follows, $Q^-(f,f)d\vec{x}d\vec{v}dt$ is the expected number of particles whose position and velocities are in the ranges $[\vec{x}, \vec{x}+d\vec{x}]$ and $[\vec{v}, \vec{v}+d\vec{v}]$ at time t, but leave these range in the time interval $[t, t+dt]$ due to a collision. This is why $Q^- \propto ff_*$, the distribution evaluated at the pre-collision velocities. The gain term is analogous, it is the number of particles whose position and velocities are outside the aforementioned ranges at time t, but enter it due to a collision. The collision kernel $B(|\vec{z}|, \cos\theta)$ varies significantly between different physical situations of interest, and in some cases has no explicit form.
In any case, with the Boltzmann collision operator, we can describe the full time evolution of a particle by the **Boltzmann equation**:

$$\partial_t f + \vec{v}\cdot\nabla_x f = Q(f,f) \tag{2.9}$$

Of interest is what physical properties are conserved for solutions of (2.9). For this we must introduce Maxwell's weak formulation.

2.2.3. Maxwell's weak formulation and conserved quantities

We note that the change of variables of $(\vec{v}, \vec{v}_*, \sigma) \to (\vec{v}', \vec{v}'_*, k)$ where $k = (\vec{v}-\vec{v}_*)/|\vec{v}-\vec{v}_*|$ has unit Jacobian and is clearly involutive, as in, reapplying the change of variables returns the original $(\vec{v}, \vec{v}_*, \sigma)$. By Assumption **4** - of microreversibility - the collision kernel B is invariant under this transformation. Additionally, the transformation $(v, v_*) \to (v_*, v)$ is also an involution with unit Jacobian, and as we have established B is invariant to this transformation (as $|v - v_*|$ remains constant under the transformation). These two invariances give rise to the weak formulation of the Boltzmann equation:

Lemma 2.2.4 (Maxwell's weak formulation)**.** *For an arbitrary continuous function of velocity, $\varphi(\vec{v})$, the following holds:*

$$\int_{\mathbb{R}^d} Q(f,f)\varphi\, d\vec{v} = \int_{\mathbb{R}^d\times\mathbb{R}^d}\int_{\mathbb{S}^{d-1}} B(\vec{v}-\vec{v}_*,\sigma)(f'f'_* - ff_*)\varphi\, d\sigma\, d(\vec{v},\vec{v}_*) \tag{2.10}$$

$$= \int_{\mathbb{R}^d\times\mathbb{R}^d}\int_{\mathbb{S}^{d-1}} B(\vec{v}-\vec{v}_*,\sigma) ff_*(\varphi' - \varphi)\, d\sigma\, d(\vec{v},\vec{v}_*) \tag{2.11}$$

$$= \frac{1}{2}\int_{\mathbb{R}^d\times\mathbb{R}^d}\int_{\mathbb{S}^{d-1}} B(\vec{v}-\vec{v}_*,\sigma) ff_*(\varphi' + \varphi'_* - \varphi_* - \varphi)\, d\sigma\, d(\vec{v},\vec{v}_*) \tag{2.12}$$

Where $\varphi' = \varphi(\vec{v}'), \varphi_* = \varphi(\vec{v}_*), \varphi'_* = \varphi(\vec{v}'_*)$.

Proof. We will omit the integration bounds to reduce unnecessary notation throughout this proof. Starting from the relation (2.10), which follows by plugging in the definition of $Q(f,f)$, we can apply the transformation $(\vec{v}, \vec{v}_*, \sigma) \to (\vec{v}', \vec{v}'_*, k)$. Note that k still runs along the unit (hyper-)sphere in $\mathbb{R}^d$.

$$\int Q(f,f)\varphi\, d\vec{v} = \int\int B(\vec{v}'-\vec{v}'_*,k)(ff_* - f'f'_*)\varphi'\, dk\, d(\vec{v}',\vec{v}'_*) = \int\int B(\vec{v}-\vec{v}_*,\sigma)(ff_* - f'f'_*)\varphi'\, dk\, d(\vec{v}',\vec{v}'_*) \tag{2.13}$$

Where in the second equality we use the invariance of the Boltzmann collision kernel. We will exploit this invariance notationally by omitting the parameters of B. Since both the right hand terms in (2.10) and (2.13) are both equal to $\int Q(f,f)\varphi d\vec{v}$, we can freely add them together to get:

$$\begin{aligned} 2\int Q(f,f)\varphi\, d\vec{v} &= \int\int B\cdot(ff_* - f'f'_*)(\varphi' - \varphi)\, dk\, d(\vec{v}',\vec{v}'_*) \\ &= \int\int B\cdot ff_*(\varphi' - \varphi)\, dk\, d(\vec{v}',\vec{v}'_*) + \int\int B\cdot f'f'_*(\varphi - \varphi')\, dk\, d(\vec{v}',\vec{v}'_*) \end{aligned} \tag{2.14}$$

The second integral involving $f'f'_*$ can be rewritten in terms of the first by reapplying the transformation. Although it is not immediately obvious, since $(\vec{v}', \vec{v}'_*, k)$ runs along all values of $\mathbb{R}^d\times\mathbb{R}^d\times\mathbb{S}^{d-1}$, we can 'relabel' the parameters to $(\vec{v}, \vec{v}_*, \sigma)$, so the first integral reads $\int Bff_*(\varphi' - \varphi)d(\vec{v}, \vec{v}_*, \sigma)$. Proceeding then with the second integral we have:

$$\int\int B\cdot f'f'_*(\varphi - \varphi')\, dk\, d(\vec{v}',\vec{v}'_*) = \int\int B\cdot ff_*(\varphi' - \varphi)\, d\sigma\, d(\vec{v},\vec{v}_*)$$

Plugging this and our earlier observation into (2.14) gives us:

$$2\int Q(f,f)\varphi d\vec{v} = 2\int\int B\cdot ff_*(\varphi'-\varphi)\,d\sigma\,d(\vec{v},\vec{v}_*)$$

Which, upon dividing throughout by 2 yields us (2.11) as required.
For the second equation, we use the transformation $(v, v_*) \to (v_*, v)$ on (2.11). We get:

$$\int Q(f,f)\varphi d\vec{v} = \int\int B\cdot ff_*(\varphi'-\varphi)\,d\sigma\,d(\vec{v},\vec{v}_*) = \int\int B\cdot f_*f(\varphi'_*-\varphi_*)\,d\sigma\,d(\vec{v}_*,\vec{v})$$

Adding the two latter integrals and dividing throughout by 2, in a similar fashion to the previous proof, gives the result (2.12) as desired. □

This weak formulation of the collision operator is often more useful than the definition provided in (2.8), as there are occasions where (2.12) is well-defined but $Q(f,f)$ is not. Moreover, from a formal point of view, for any solution f of the Boltzmann equation (2.9) we have:

$$\frac{d}{dt}\int f(t,\vec{x},\vec{v})\varphi(\vec{v})\,d\vec{x}\,d\vec{v} = \int Q(f,f)\varphi\,d\vec{x}\,d\vec{v} \tag{2.15}$$

where we used our previous observation that the transport operator does not contribute. So Maxwell's weak formulation allows us to describe the change of $\int f\varphi d\vec{v}$ with respects to time. Additionally, if f satisfies the equation (2.15) for all functions $\varphi \in C(\mathbb{R}^d)$, it is called a **weak solution** to the Boltzmann equation, as in every macroscopic sense it is indistinguishable from a solution of (2.9). This notion of weak solutions (or forms or derivatives) crops up a lot in analysis as it allows for a relaxation of the more stringent requirements (solutions, differentiability, etc.). Nonetheless, it is clear from the shape of (2.12), that if φ satisfies the equation:

$$\forall(\vec{v},\vec{v}_*,\sigma)\in\mathbb{R}^d\times\mathbb{R}^d\times\mathbb{S}^d,\quad \varphi(\vec{v}')+\varphi(\vec{v}'_*)=\varphi(\vec{v})+\varphi(\vec{v}_*)$$

Then $\frac{d}{dt}\int f\varphi d\vec{v} = 0$, for solutions of the Boltzmann equation. Under weak conditions [7, pgs. 36-42], solutions of the equation for φ are only linear combinations of the so-called **collision invariants**:

$$\varphi(\vec{v}) = 1, v_i, |\vec{v}|^2, \qquad 1\le i\le d$$

Which we would expect from the conservation of kinetic energy and momenta (1 is just a constant function, and so trivially satisfies the equation). The corresponding conserved macroscopic observables are namely:

$$M = \int_{\mathbb{R}^d}\int_{\mathbb{R}^d} f(t,\vec{x},\vec{v})\,d\vec{v}\,d\vec{x} \qquad \text{(mass)} \tag{2.16}$$

$$\vec{P} = \int_{\mathbb{R}^d}\int_{\mathbb{R}^d} \vec{v}f(t,\vec{x},\vec{v})\,d\vec{v}\,d\vec{x} \qquad \text{(momentum)} \tag{2.17}$$

$$E = \int_{\mathbb{R}^d}\int_{\mathbb{R}^d} |\vec{v}|^2 f(t,\vec{x},\vec{v})\,d\vec{v}\,d\vec{x} \qquad \text{(energy)} \tag{2.18}$$

2.3. The Boltzmann collision kernel for hard spheres

In the following section, we will formally derive the Boltzmann collision kernel for hard sphere interactions in 3D space. To this end we will need to use a **two-particle distribution function** $f^{(2)}(t,\vec{x},\vec{v},\vec{x}_*,\vec{v}_*)$. We will be following the work of Cercignani [7, pgs. 19-23] as the basis of this derivation. We suppose the gas consists of N hard spheres, each with radius r. Let us examine how the loss term can be derived Q^-.

As elaborated earlier, $Q^- d\vec{x}d\vec{v}dt$ gives the expected number of particles with position between $\vec{x}$ and $\vec{x}+d\vec{x}$, and velocities in $[\vec{v},\vec{v}+d\vec{v}]$ that leave these ranges due to a collision in a time interval between t and $t+dt$. If the first particle, which we will label particle 1, is in the position and velocity ranges described earlier, any collision with any particle will send it out of the range. So to calculate Q^- we simply need to count the expected collisions of particle 1 with the remaining $N-1$ particles, which are all identical, as by assumption **1** we discard non-binary collisions . So $Q^- = (N-1)q^-$, where q^- is the expected number of collisions with a single fixed particle, say particle 2.

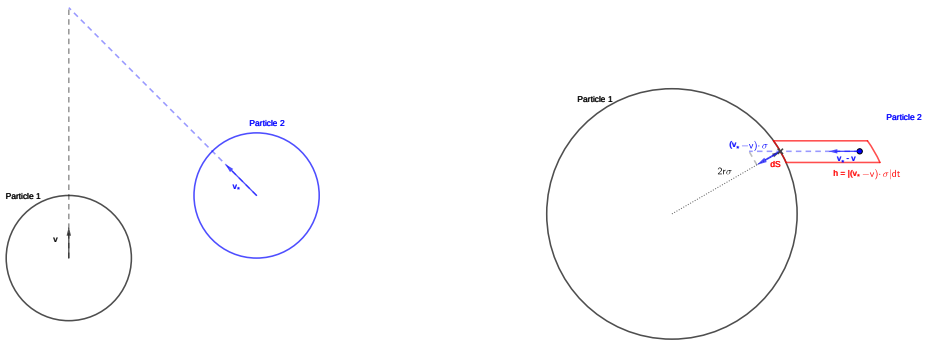

(a) (b)

Figure 2.1: (a) A plot of an example collision between particles 1 (black) and 2 (blue) and (b) the same collision with the changes in frame of reference described below. The slanted cylinder is the enclosed red region. Both plots made using GeoGebra

To count these collisions, we will employ the following trick: we imagine the first particle (i.e. 1 with position $\vec{x}$ and velocity $\vec{v}$) as a sphere of radius $2r$, and the second colliding particle (2, with position $\vec{x}_*$ and velocity $\vec{v}_*$) as a point mass. Moreover, we will change our frame of reference so that the first particle is at rest and the second particle has a velocity $\vec{v}_* - \vec{v}$.

At the moment of collision, we expect $\vec{x}_* = \vec{x} + 2r\sigma$, where $\sigma \in \mathbb{S}^2$, so the momentum distribution of particle 2 at the moment of collision (as a function of v_*) is $f^{(2)}(t, \vec{x}, \vec{v}, \vec{x} + 2r\sigma, \vec{v}_*)$. If we wish to count the collisions on an infinitesimal area $(2r)^2 d\sigma$ on the sphere of radius $2r$, then the second particle collides in the time interval if and only if it lies in a slanted cylinder with height $|(\vec{v}_* - \vec{v}) \cdot \sigma| dt$ and base $4r^2 d\sigma$, see Figure 2.1. So the number of collisions of particle 2 with particle 1, occurring on an area $4r^2 d\sigma$, when particle 1's coordinates lie in the ranges $[\vec{x}, \vec{x} + d\vec{x}], [\vec{v}, \vec{v} + d\vec{v}]$ and particle 2 lies on$\vec{x}_* = \vec{x} + 2r\sigma$, with velocity in $[\vec{v}_*, \vec{v} + d\vec{v}_*]$, is given by:

$$f^{(2)}(t, \vec{x}, \vec{v}, \vec{x} + 2r\sigma, \vec{v}_*) |(\vec{v}_* - \vec{v}) \cdot \sigma| 4r^2 \, d\sigma d\vec{x} d\vec{v} d\vec{v}_* dt$$

Integrating over all possible velocities $\vec{v}_*$, and possible collision locations on the sphere (which will be a hemisphere $\mathbb{S}^2_-$, where $(\vec{v}_* - \vec{v}) \cdot \sigma < 0$ so the particles are moving towards each other), gives us:

$$q^- d\vec{x} d\vec{v} dt = d\vec{x} d\vec{v} dt \int_{\mathbb{R}^3} \int_{\mathbb{S}^2_-} f^{(2)}(t, \vec{x}, \vec{v}, \vec{x} + 2r\sigma, \vec{v}_*) |(\vec{v}_* - \vec{v}) \cdot \sigma| 4r^2 \, d\sigma \, d\vec{v}_*$$

Evidently the loss term Q^- then reads:

$$Q^- = (N-1) 4r^2 \int_{\mathbb{R}^3} \int_{\mathbb{S}^2_-} |(\vec{v}_* - \vec{v}) \cdot \sigma| f^{(2)}(t, \vec{x}, \vec{v}, \vec{x} + 2r\sigma, \vec{v}_*) \, d\sigma \, d\vec{v}_*$$

Now, we recall assumption **1**, namely the dilute gas assumptions. Since $Nr^3 \ll 1$ and $Nr^2 \simeq 1$, we will take a scaling limit $N \to \infty, r \to 0, Nr^2 \to C < \infty$. Absorbing constants, and assuming continuity on $f^{(2)}$, we get:

$$Q^- \approx C \int_{\mathbb{R}^3} \int_{\mathbb{S}^2_-} |(\vec{v}_* - \vec{v}) \cdot \sigma| f^{(2)}(t, \vec{x}, \vec{v}, \vec{x}, \vec{v}_*) \, d\sigma \, d\vec{v}_* \tag{2.19}$$

We note the only σ dependent terms now is the absolute value term, which will be positive regardless of the sign of the inner product. Hence we can integrate over the whole $\mathbb{S}^2$, scaled down by $\frac{1}{2}$. The scaling limit we used to derive this expression is known as the **Boltzmann-Grad limit**, and describes the asymptotic regimes wherein the Boltzmann equation (2.9) is expected to accurately describe particle dynamics.
Whilst equation (2.19) is starting to look like what we ultimately desire, it is unfortunately in terms of the two-particle distribution $f^{(2)}$, and so we are still none the wiser on how f evolves due to collisions. To this end, we recall Assumption **5**, of **molecular chaos**. Boltzmann's insight was as $N \to \infty$, for any two fixed particles a collision between the two is a rare event, and so we consider them as random events, consisting of an interaction between randomly chosen particles. Moreover, since we assume the pre-collision velocities of the two particles are uncorrelated, we have:

$$f^{(2)}(t, \vec{x}, \vec{v}, \vec{x}_*, \vec{v}_*) = f(t, \vec{x}, \vec{v}) \cdot f(t, \vec{x}_*, \vec{v}_*)$$

And from this result, substituted into (2.19), gives us an expression we are familiar with:

$$Q^- = \frac{C}{2}\int_{\mathbb{R}^3}\int_{\mathbb{S}^2} |(\vec{v}_* - \vec{v})\cdot\sigma| f(t,\vec{x},\vec{v})\cdot f(t,\vec{x},\vec{v}_*)\, d\sigma\, d\vec{v}_* \tag{2.20}$$

We see that this expression is of the form of $Q^- = \int\int B(\vec{v}_* - \vec{v},\sigma) f f_* d\sigma d\vec{v}_*$, and we conclude that the collision kernel for hard-spheres is given (up to a constant) by:

$$B(\vec{v}_* - \vec{v},\sigma) = |(\vec{v}_* - \vec{v})\cdot\sigma|, \qquad B(|\vec{v}_* - \vec{v}|,\cos\theta) = |\vec{v}_* - \vec{v}||\cos\theta|. \tag{2.21}$$

The two expressions are identical, but the second more clearly indicates how the collision kernel is a function of solely the absolute difference in speeds and the deviation angle θ.

A few remarks can be said about this derivation process. Firstly, we will discuss the derivation of the gain term Q^+. Whilst the procedure is identical in many of the steps, except that σ is integrated over $\mathbb{S}^2_+ = \{\sigma \in \mathbb{S}^2 : (\vec{v}_* - \vec{v})\cdot\sigma > 0\}$, at some point we must rewrite the expression in terms of the post-collision velocities. This comes before the Boltzmann-Grad limit, where we assume on physical grounds that $f^{(2)}$ is continuous at a collision, i.e.:

$$f^{(2)}(t,\vec{x},\vec{v},\vec{x}_*,\vec{v}_*) = f^{(2)}(t,\vec{x},\vec{v}',\vec{x}_*,\vec{v}'_*)$$

It should then be clear how $f'f'_*$ appears in the gain term, by again applying the scaling limit and using the molecular chaos assumption. A full treatment of the derivation of the gain term can be found in Cercigani's work [7].
Secondly, we find that the molecular chaos assumption is a strong one. Coupled with the continuity assumption of $f^{(2)}$ at the time of collision, it is logical to conclude that the uncorrelated pre-collision velocities give rise to *uncorrelated post-collision velocities*. But this is nonsense from a rigorous probablistic standpoint: the moment the particles collide their velocities *must* be correlated. An interpretation of the assumption, then, is that these correlations are negligible in the scaling limit.
Lastly, though we started this derivation explicitly in a 3 dimensional space, we only used this fact in the scaling limit. As such, we find that much of the same analysis can be reused to conclude that in *any* dimension, the Boltzmann collision kernel has the shape of (2.21) for hard sphere elastic collisions.

2.4. Fokker-Planck equations

Another set of kinetic equations that describe the evolution of certain gas processes is the Fokker-Planck equation. Described in 1914 by Dutch physicist Adriaan Fokker [15] and then in 1917 by the well-known German Physics Nobel Prize winner Max Planck [27], the equation is a diffusive model. Based on the assumption that the particle dynamics can be treated as Brownian motion, and that the process is independent of the past, i.e. a Markov process, it appears in many diverse fields of mathematics: economics, information theory, and kinetic theory, to name a few. The full derivation in the physical context is handled in detail by the comprehensive review paper by Chandrasekhar [8, pgs. 31-33]. The linear kinetic Fokker-Planck equation, which will be of interest in future chapters, reads as follows:

$$\partial_t f + v\cdot\nabla_x f = \nabla_v\cdot(\sigma\nabla_v f + \beta\vec{v}f) \tag{2.22}$$

Where as before ∇_x represents the gradient in the position coordinates, and ∇_v the gradient in the velocity coordinates. $\sigma > 0$ is known as the **diffusion** coefficient, and $\beta \geq 0$ is known as the **friction** coefficient. In the case of spatial homogeneity, we see that an equilibrium distribution of f is the Maxwellian velocity distribution. Indeed, this becomes clear by rewriting (2.22) into:

$$\partial_t f = \sigma\nabla_v\cdot\left(\nabla_v f + \frac{\beta}{\sigma}\vec{v}f\right)$$

Then the Maxwellian distribution below, for some normalization constant C, is an equilibrium distribution:

$$f(t,\vec{v}) = Ce^{\frac{-\beta|\vec{v}|^2}{2\sigma}} \implies \nabla_v f = -\frac{\beta}{\sigma}\vec{v}Ce^{\frac{-\beta|\vec{v}|^2}{2\sigma}} = -\frac{\beta}{\sigma}\vec{v}f \implies \partial_t f = 0 \tag{2.23}$$

We will derive, in Chapter 5, that the dynamics of the piston in a spatially homogeneous environment, located on a mathematical torus, under a certain scaling limit (the grazing collision limit), can be accurately described by a Fokker-Planck-type equation, namely:

$$\partial_t f = \nabla_v\cdot(|v|\nabla_v f + \vec{v}|v|f) \tag{2.24}$$

A more detailed analysis of solutions of this equation and their convergence to equilibrium can be found in Section 4.2.

3

Computer simulations

We will first outline previous work done in simulating the adiabatic piston problem, then introduce a new approach for computer simulations of this sort, with a relevant discussion on optimal running times. The implementation of this algorithm led to two different approaches discussed, and then we experimentally determined what the optimal parameters are for the algorithm, and how they scale with N the number of particles. Future improvements to the algorithm are handled briefly at the end. We make use of standard notation for algorithmic analysis, with $f(n) = \mathcal{O}(g(n))$ meaning that there exists a constant $n_0, c > 0$ such that for all $n \geq n_0, f(n) < c \cdot g(n)$, $f(n) = \Omega(g(n))$ meaning that there exists a constant $n_0, c > 0$ such that for all $n \geq n_0, f(n) > c \cdot g(n)$. Hence, $f(n) = \mathcal{O}(g(n))$ means that f is bounded above by (a multiple of) $g(n)$ as $n \to \infty$, and Ω denotes a bound from below. We also note that the code is publicly available on https://github.com/Blasylf/BEP .

3.1. Prior work

Due to the curious nature of the adiabatic piston paradox, there have been multiple simulations concerned with the different characteristics and regimes of the scenario [6, 9, 21]. In all of them, the piston is perturbed from its initial rest state to an unstable oscillatory regime (assuming the pressures $P_1 \neq P_2$ are not equal). This regime stabilizes to a decaying oscillatory regime, where the piston moves to ensure mechanical equilibrium. Afterwards, once achieving this intermediate equilibrium, the piston relaxes further until equal temperatures are reached over a long time frame. This can be clearly seen in Figure 3.1.

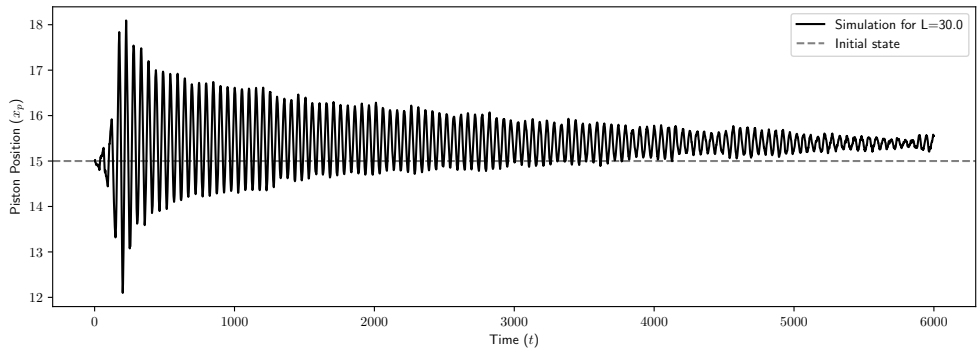

Figure 3.1: A typical plot of piston position over time, for unequal beginning temperatures and pressures ($T_1 \neq T_2, P_1 \neq P_2$). Using the same configuration as [9], the piston is in a cylinder of length $L = 30$, with $N/2 \approx 13500$ particles on either side of the piston. Zoomed in portions of this plot can be found in Fig. 3.2

First we have Chernov and Lebowitz's simulation [9]. We will base our simulation work on this paper, and so will be handling it in detail in the algorithmic sense in Section 3.1.2. Nonetheless, in [9], they were

interested in confirming the **hydrodynamics limit** through means of a large simulation, in the 'simple' scenario of particles that only interact with the piston (and so not with each other) through elastic collisions. They considered in effect a one dimensional cylinder of length L, and observed the limit as $L \to \infty$. This was initially motivated by prior work [10] that derived deterministic equations for the piston's position (as a Ornstein–Uhlenbeck process, which is both a Gaussian and a Markov process - details of which can be found in [25, Ch. 9]), ignoring the case of particle re-collisions, where a particle collides twice or more with the piston. Of course, the finite cylinder forces re-collisions, and these give rise to auto-correlations that ruin the Markov property as they build up with each re-collision [10]. In order to accurately describe the limiting regime through means of computer simulations, they ran a comprehensive model for $N = 27 \cdot 10^6$ particles, for a long time period (roughly $\sim 10^3$ collisions per particle).

Next we have Cencini et al.'s work [6]. In their paper, they derive a set of macroscopic equations for the adiabatic piston in the **thermodynamic limit** of $N, m_p, L \to \infty$, where N is the number of particles, L the length of the cylinder, and m_p the mass of the piston (the masses of the particles remain fixed). They then verify these derivations through means of a computer simulation, on two different types of gas. Since they posit a few assumptions in their derivation, the second type of gas explicitly satisfies those assumptions. Curiously, it is modelled through constantly 'resampling' the gas from the macroscopic variables. That is to say, an initial configuration of the system is generated, corresponding to the macroscopic variables, and develops (with no particle-particle interactions) until the first collision with the piston. The transferred kinetic energy is then used to determine the new temperatures across both sides of the piston, and then the particles are re-sampled according to this new macroscopic configuration. Whilst the number of particles wasn't particularly large at $N = 10^3$, the simulations were run until $t \sim 10^7$, and then re-run ~ 100 times to take an average across multiple runs. Therein they confirm that the second gas type agrees with their model, but the standard ideal gas does not when the total mass ratio is too small (it converges far slower to an equilibrium state).

Lastly of interest is Mansour et al.'s work [21]. They consider the cylinder in **2 dimensional** space, and approached the entire problem, in the theoretical sense, from the hydrodynamical perspective. There they used the molecular dynamics simulation and compared them against numerically solved hydrodynamic equations. Moreover, they take a limit as the piston mass $m_p \to \infty$ to derive a set of macroscopic equations for the piston's dynamics, and use the simulation to test these results.

3.1.1. Introduction of discrete model

In order to describe the time evolution of a kinetic system in the adiabatic piston context, we simulate N individual particles, each of mass m. Recall in Chapter 2 that the piston is found in a cylinder, of length L, and cross-sectional area A. Often times it is convenient to reduce the problem to one dimension, as the piston can only move along the axis of the cylinder. Then the piston position and velocity $(x_p, v_p) \in [0, L] \times \mathbb{R}$ are strictly one dimensional. We must also take into account the piston mass m_p. Returning to the N particles, we split these into N_1 particles left of the piston, and N_2 particles right. For all of these, we must track their velocities $(x_i, v_i) \in [0, L] \times \mathbb{R}, 1 \leq i \leq N$. For the simplest model, which we will be using here on out, the particles solely interact through **elastic collisions** with the **piston**. This means between collisions, x_i can be recovered directly from v_i, through simply:

$$x_i(t) = x_i(t_0) + v_i(t_0)(t - t_0), \tag{3.1}$$

where t_0 is the time since last collision for particle i with the piston. If particle i collides with the piston, its new velocity can be computed by:

$$v_i' = \frac{m - m_p}{m + m_p} v_i + \frac{2m_p}{m + m_p} v_p, \quad v_p' = \frac{2m}{m + m_p} v_i + \frac{m_p - m}{m + m_p} v_p, \tag{3.2}$$

where once again the primes denote the post-collision velocities. Then there is the question of boundary conditions. Since the model has been reduced to one dimension, there is only two types of boundary conditions possible:

1. Elastic collisions with the cylinder walls at $x = 0$ and $x = L$. In this case, particle velocities simply get reflected $v_i' = -v_i$.

2. Periodic boundary conditions, wherein a particle upon reaching $x_i(t^-) = 0$ (or L respectively), continues with the same velocity $v_i(t)$ from the other side $x_i(t^+) = L$ (or 0 respectively).

The computer model then calculates the velocities and positions of the particles and pistons (representing $2N+2$ variables) according to the collision laws (3.2) and boundary conditions, from an initial time $t=0$ up to some finite time t. The initial configuration also needs to be given as an input for the computer model. Since it is generally unwieldy to specify all $2N$ parameters for the particles, it is common to simply describe the initial **probability density function** $f_0(x,v)$, and then take $2N$ samples of it. However, in most simulations and indeed in later parts of this thesis for theoretical work, we consider only the spatially homogeneous case. In this regime, the positions of particles are distributed uniformly across the cylinder (or, eventually, across either the interval $[0, x_p(t=0)]$ for particles on the left side of the cylinder, and $[x_p(t=0), L]$ for the right). Then f_0 becomes solely a probability density function over velocities, and such N samples are taken to determine the particle velocities v_i.
So all in all, we have the following degrees of freedom for input:

- The mass ratio $\frac{m}{m_p}$ exclusively determines the shape of the collision laws in (3.2).
- The number of particles N_1 on the left of the piston, and N_2 on the right.
- The initial velocity distribution $f_0(v)$ for the particles, from which the initial particle velocities are randomly generated.
- Likewise, the initial velocity and position of the piston, of which it is customary to take $x_p(t=0)=\frac{L}{2}$ and $v_p(t=0)=0$.
- The length of the cylinder L.
- The boundary conditions, either specular reflection or periodic.

From this construction, it is clear to see that N_1, N_2, the masses, and total kinetic energy are conserved. Let us gain some insight on the macroscopic variables outlined in Section 2.1 from the simulation variables described above. Since we have an ideal gas setting - elastic collisions, gas particles modelled as hard spheres (of radius $r=0$!) - we can link the temperatures T_1, T_2 to the average kinetic energy of the molecules. Indeed, we have the well-known relation for ideal gases:

$$\frac{1}{2}m\langle v^2\rangle = \frac{3}{2}k_B T,$$

where $\langle v^2\rangle = \frac{1}{N}\sum_{i=1}^{N} v_i^2$ is the sample average of v^2 and k_B is the Boltzmann constant ($1.38\cdot 10^{-23} J/K$) . We will denote $\langle v^2\rangle_{1,2} = \frac{1}{N_{1,2}}\sum_{i=1}^{N_{1,2}} v_i^2$ the sample averages for the left and right sides respectively. To avoid dealing with k_B, we set it to 1 (which is equivalent to taking the masses of the particles in the order of k_B). Then we have:

$$m\langle v^2\rangle_1 = 3T_1, \quad m\langle v^2\rangle_2 = 3T_2$$

This result can also be recovered directly from the equipartition theorem. To derive the pressures, one can use the relation $PV = Nk_bT$. Since we have $V_1 = Ax_p$, $V_2 = A(L-x_p)$, we get:

$$P_1 = \frac{N_1 T_1}{Ax_p} \propto \frac{N_1 m\langle v^2\rangle_1}{x_p}, \quad P_2 = \frac{N_1 T_1}{A(L-x_p)} \propto \frac{N_1 m\langle v^2\rangle_2}{L-x_p}.$$

In the case that $x_p = \frac{L}{2}$, equal pressures only holds if $N_1\langle v^2\rangle_2 = N_2\langle v^2\rangle_2$ which, as noted in Chapter 2, is a looser condition to equal temperatures. If we have additionally that $N_1 = N_2$, then equal pressures and equal temperatures occur simultaneously, and so the situation is of no particular interest. Due to the random nature of sampling the velocities, in general $\langle v^2\rangle_1 \neq \langle v^2\rangle_2$ and so every computer simulation deals with a state that is not in thermal equilibrium.

3.1.2. Chernov and Lebowitz's simulation

As mentioned previously, Chernov and Lebowitz [9] were interested in the scaling limit as $L\to\infty$. To this end, they fixed some of the degrees of freedom outlined before as functions of L. To ensure a distinction between the mechanical (equal pressures) equilibrium and thermal equilibrium regime, they sampled N_1, N_2 from a Poisson process with parameter $L^3/2$. As a consequence, $N\sim L^3$ and $N_1\approx N_2$. Moreover, they fixed the piston mass to scale as $m_p = 2mL^2$ and hence the mass ratio is given by $\sim L^{-2}$. They used hard boundaries and an

initial piston state of $v_p(0) = 0, x_p(0) = L/2$. The scaling of N, m_p with respects to L was chosen so that, if the particles are initially distributed with velocities of order $\mathcal{O}(1)$ and density $\mathcal{O}(1)$, the acceleration of the piston remains fixed at order $\mathcal{O}(1)$. Then, under the hydrodynamic scaling limit $\tau = t/L, y_p(t) = x_p(t)/L$, one finds that the piston satisfies hydrodynamic questions so long as $M \sim N^\alpha$ for $\alpha \in (0,1)$ [10]. They had also shown, for particular velocity distributions, these solutions are unstable with the initial conditions provided. One of these velocity distributions is a **bimodal uniform distribution**, i.e.:

$$f_0(v) = \begin{cases} p_0, & v_{\min} \le |v| \le v_{\max} \\ 0, & \text{otherwise} \end{cases} \tag{3.3}$$

For some normalizing constant p_0. In the case of the simulation in [9], $v_{\min} = 0.5, v_{\max} = 1$. What was not clear from the theoretical point of view is for how long the hydrodynamic equations represented an approximate solution to the evolution of the particle system, for large N, hence motivating the intensive computer simulation [4]. In the simulation, L was at most 300, giving rise to $N = 27 \cdot 10^6$ particles. Their numerical results studied also how long the unstable regime lasted ($\sim L \log L$) and how long the relaxation to the equilibrium took ($\sim L^{7/2}$). The instability and relaxation was observed in our recreation, see namely Figure 3.2.

3.2. An efficient algorithm for particle collisions

As we saw in the previous section, some of the computer simulations involve a lot of particles or are run for a long amount of time. As such, it is in our best interest to find an efficient algorithm to simulate the procedure.

3.2.1. Initial approaches

In recreating [9], we found that the computations for $L = 300$ was quite slow. Naively, a natural approach for many trained in numerical methods is to discretize time, and integrate over a time step Δt. Since in our case we have point masses, one can check during a time-step if a particle is going to collide with the piston, and handle it accordingly. However, this raises many complications. Firstly, if many particles are identified as going to collide with the piston, then there is the matter of picking which one collides first, as the order of collision matters. Worse still, after the first collision, the new piston velocity v_p' may be such that the initially calculated order is completely wrong. Moreover, this method cannot detect if a particle collides *twice* (or more) in a time step.

A smarter approach, is noting the fact that between collisions the system is fully deterministic from some initial position and the velocities. As mentioned before, the position at an arbitrary time can then be recovered by (3.1). So it would be logical to simply determine the first particle to collide with the piston, and then update the system accordingly to the new time. The problem with this, however, is that after each collision, the piston velocity changes, and so the first particle to collide has to be redetermined. If N_c is the number of collisions, then we would expect the computation time to scale with $\mathcal{O}(N_c N)$. We can quantify this further if we assume that the particle velocities are on the order of $\langle |v| \rangle$ (i.e. close to the sample mean in absolute value), the piston starts at rest in the middle and the situation is such that:

$$\forall\, t \ge 0 : \quad |x_p(t) - x_p(0)| \ll L, \quad |v_p(t)| \ll \langle |v| \rangle$$

i.e. the oscillations of the piston are small compared to the particle motion, then it is reasonable to assume that the time t_* between a particle's collision is given by $t_* \sim \frac{L}{\langle |v| \rangle}$ (if the piston is fixed at $L/2$, the particle must travel to the wall and back to collide again). Hence the number of collisions would scale with $N_c = N t / t_*$, and so the naive approach of recalculating the collision times for every collision would cost

$$\mathcal{O}(N^2 t \langle |v| \rangle / L) = \mathcal{O}(N^2)$$

Which is quadratic in N, and so not ideal. What would be the ideal algorithm, then? Well, if we take the strategy of updating the system due to the collisions, any algorithm would have to run at least as often as there are collisions, so an optimal algorithm has complexity $\Omega(N_c)$. Indeed, if the output of the program includes the ordered collision times, then one could argue that an optimal algorithm has complexity $\Omega(N_c \log N)$. [29]

3.2.2. Description of algorithm

Fortunately, we find an improved algorithm in [29]. Instead of trying to recalculate the collision times for every particle after every collision, instead we group up the particles (and piston) into **cells**, and only recom-

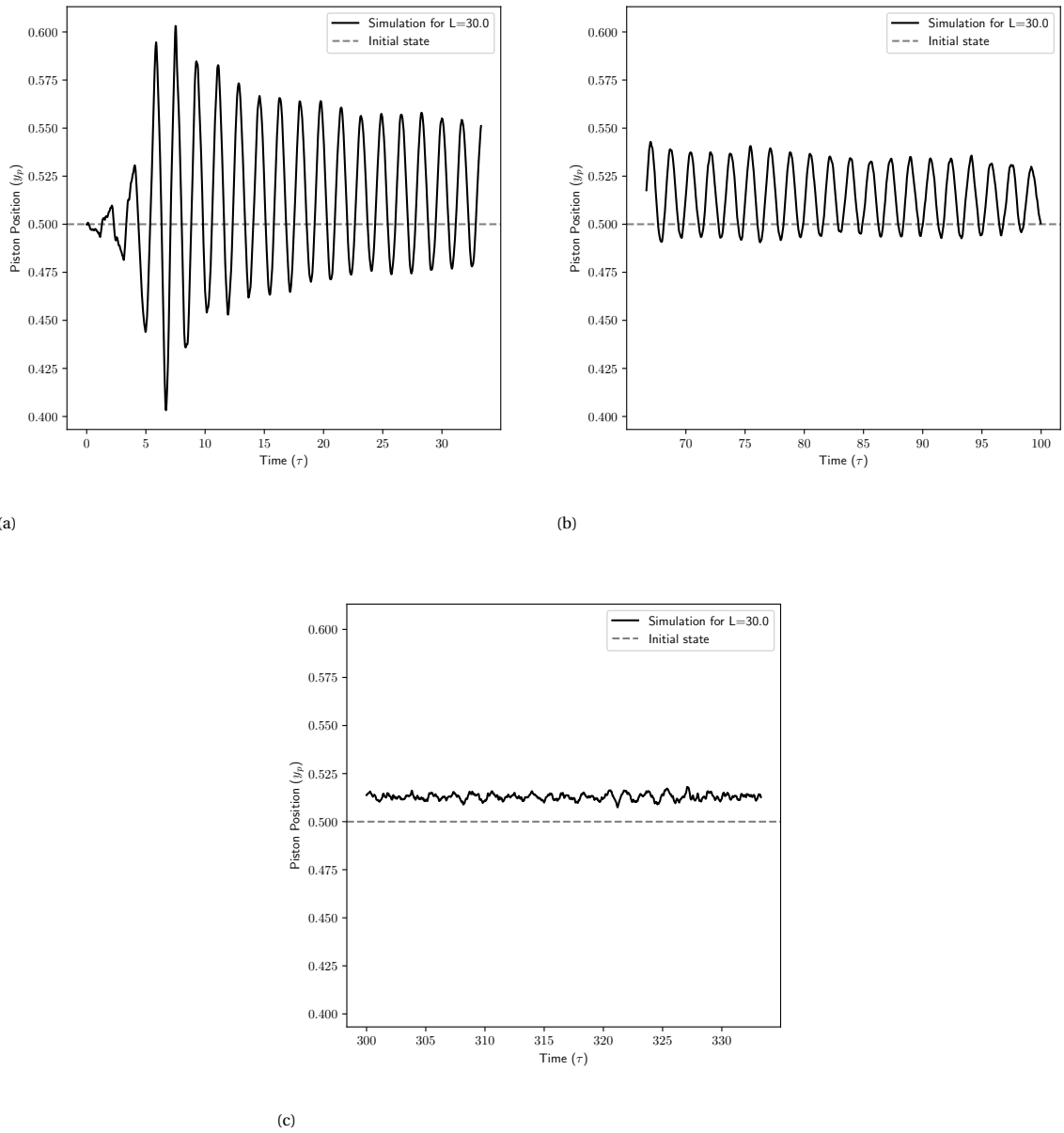

Figure 3.2: Above, plots of the re-scaled piston position $y_p = x_p/L$ over re-scaled time $\tau = t/L$ using the same configuration as [9]. Here $L = 30$ and so $N \approx 27000$. (a) The piston begins to oscillate with an exponential amplitude growth, which then quickly stops to give rise to a damped oscillation. (b) These damped oscillations then persist for a long time in comparison to the unstable period and (c) after sufficiently long times, the piston enters a noisy regime.

pute the collision times for particles in the neighbouring cells of the collision (which, in our case will always be the piston). In the case of [29], these cells are uniform in length, and so if we have m_c cells (not to be confused with mass), then each cell with have a length $l = L/m_c$. In the higher d-dimensional case, the side-lengths of the cells will be $l = Lm_c^{-1/d}$ assuming the simulation's spatial space is $[0, L]^d$. Whilst these cells cut down on the computational costs for collisions, some computation time must be spent on keeping track of which particle belongs to which cell. Moreover, we incur a minor memory cost on storing the **cell structure**

Formalizing this idea, we have then an **event queue**. Each particle corresponds to one event in the queue, and there are two types of events:

1. **Collision** events, in which the particle in question collides with the piston. If this happens, both the

particle and the piston's velocities need to be updated in accordance to the collision laws (3.2), with their positions set to the point of impact.

2. **Transfer** events, in which a particle moves from one cell to another (adjacent) cell. If this happens, the particle's position needs to be updated.

The event queue is implemented as a heap, and ordered by the **system time** of the occurrence of the event (so not necessarily the time until the event happens). One can note that each event only leads to the updating of one or two objects (the particle, and eventually the piston). Indeed, we can **delay the update** of the whole system by keeping track, for each particle, the time since the last event (involving said particle) t_0. Once again, (3.1) recovers the position of the particle at time t, if needed, for example, to compute collision times. However, in doing so, it is critical that the queue is ordered by the system time of the event occurring, and not the event duration (as otherwise slow-moving particles will never get updated, without forcing an update across the system, which brings us back to the non-optimal algorithm). In the case of a transfer event, we also need to ensure that we are not approaching the piston, otherwise we need to compute the collision time. So in general, we get an algorithm of the form:

- Step 1: Find the next event in the event queue.
- Step 2: Handle the event
  - If it is a collision event, update the relevant velocities
  - If it is a transfer event, update the cell structure
- Step 3: Compute the next transfer time for the particle corresponding to the event
- Step 4: Compute the next collision time with particles in the appropriate neighbouring cells
- Step 5: Adjust the position of the event and, in the general case, the other colliding particle's event in the queue (in our case it is always the piston).
- Step 6: Return to Step 1

We note that Step 4 is slightly less computation work than it initially seems. If the event is a transfer event, then we only need to compute the collision times for the 'new' neighbouring cells, see for example Figure 3.3 from [29].

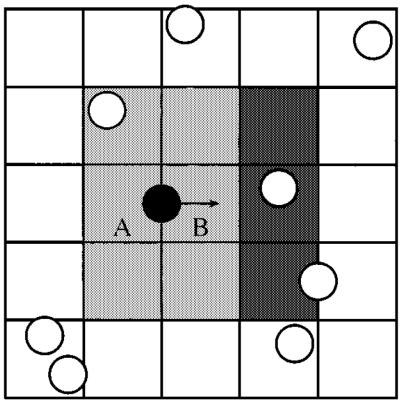

Figure 3.3: The black particle just transferred from cell A to cell B, and so only needs to compute collisions in the dark-shaded cells, as it already computed collisions in the lightly shaded cells. Taken from Sigurgeirsson et al., 2001 [29, Fig. 3]

We have, up until this point, avoided mentioning boundary conditions. In reality, they are not that difficult to implement in this system. Under the two types of boundary conditions mentioned in Section 3.1.1, we find that it is sufficient to treat the boundary as a collision event. In the case of hard boundaries, these are in fact collisions, and in the case of periodic boundaries, the particles are transferred to the other side of the piston (and their respective cell position updated).

We will now remark the following significant divergence from [29]. Since we only have the colliding piston, there is no need to consider collision events as pairs (and so avoiding the "check" events described in the paper). Moreover, we need to handle the piston differently, as it is the only particle that can transfer between cells and get collided *on*. In our implementation, we give the piston an event that is *exclusively* a transfer event, with collisions against the piston handled by the particles' collision events. More details on how this algorithm is implemented will be elaborated in Section 3.3.

3.2.3. Running time analysis

Following the steps of [29], we see that:

- Step 1 is a single operation (as the event queue is a heap, so the smallest element is always 'on top')
- Steps 2 & 3 involves a constant number of operations
- Step 4 involves a constant number of operations for each particle in the neighbouring cells. If we denote $n_s(i)$ as the number of particles in the neighbouring 3 (in the 1D case) cells, at the occurrence of event i, then this step incurs $n_s(i)-1$ operations
- Step 5 involves at most $\log N$ operations.

Combining these, we find that the total computational cost satisfies:

$$\mathcal{O}\left(\sum_{i\in\text{events}}(1+n_s(i)+\log N)\right)$$

If we assume a uniform spatial distribution, then the number of particles per cell is (in the 1D case) N/m_c, where again m_c is the number of cells. So we can expect $n_s(i)=\mathcal{O}(N/m_c)$. We can then rewrite the sum over the events as a multiplication over the expected number of events. This expectation can be bounded from above as the expected number of collisions N_c and the expected number of transfers, N_t. In the general case, for particle-particle collisions, Sigurgeirsson et al. derive that the average complexity of the algorithm satisfies:

$$\mathcal{O}\left(\left(1+\log N+\frac{N}{m_c}\right)\left(\sigma_c\frac{N}{L}+\frac{m_c}{L}\right)\mathbb{E}[|v|]Nt\right) \tag{3.4}$$

Where σ_c is the collision cross-section. We note that $\mathbb{E}[|v|]$ denotes the expected absolute particle velocity. In the second pair of brackets one sees clearly the expected number of collisions and transfers, respectively. From (3.4), [29] concludes that the ideal number of cells should scale with N, so that $N/m_c\sim 1$ in the first brackets and equivalently the number of transfers scales with the number of collisions in the second set of brackets. Under this configuration, we would expect that (3.4) simplifies to:

$$\mathcal{O}\left((1+\log N)\frac{N}{L}\mathbb{E}[|v|]Nt\right)=\mathcal{O}\left(N^2\log N\right)=\mathcal{O}(N_c\log N)$$

Where in the last step we note in 1D, particle-particle collisions gives $N_c\sim N^2$. In our case, however, we have only the piston colliding and so the computing time should scale differently in N. In particular, the expected number of collisions should scale more slowly, but Step 5 should incur a larger cost as every particle is "partners" with the piston. Due to time constraints, however, the exact details of this scaling was not confirmed.

3.3. Implementation

We implemented the algorithm outlined in Section 3.2.2, under the variable constraints given in 3.1.2 (as we were interested in reproducing the results of [9]). The spatial positions are distributed uniformly over $[0,L]$ and the velocity distribution was of the form (3.3), with $v_{\min}=0.5, v_{\max}=1$. These distributions were sampled using a random number generator known as the Mersenne Twister (for more details see [23]).
As mentioned previously, the algorithm in Section 3.2.2 requires an event queue which needs to act as a heap. Each event corresponds 1-1 to a particle, so naturally it would make sense to have one point to the other. We managed to implement this by keeping the list of particles fixed, and having each particle keep track of its own events. The event queue, then, would order a set of *pointers* to the events. The associated particle to an event can be recovered as each event stores the *index* of the particle in the particle list associated to the event.

The exceptional case is the piston. Since the piston is handled differently in terms of events (it only transfers between cells, collision computations are 'offloaded' to the particles), its event is stored separately, and points to an index of -1 to identify it as the piston.
The cell structure was relatively easy to implement, being a list (of length m_c) of lists containing the indices of the particles. As mentioned earlier, boundary conditions were handled as collision events, with a flag `.wall` to indicate if the event was a collision.

Due to the nature of floating point precision, some adjustments had to be made. Rounding errors could mean that if one computed the position of impact for a particle and a piston by (3.1) separately, one would find $x_p(t) \neq x(t)$ at the time of impact. Fortunately this was not that bad in most cases, if v', v had opposite signs (because then the particle would transfer back to its correct positions, albeit at a slightly slower pace). The problem became more serious if the piston was on the boundary between two cells, as it could lead to a particle erroneously thinking it is in the right cell, and transferring further rightwards or re-colliding with the piston, when it should remain in the left cell. In general, these errors led to particles phasing through the piston, but were fixed by simply forcing the position of the particle to match that of the piston at the time of impact, and forcing the two to lie in the same cell.

A bigger problem, however, was Step 5. Indeed, whenever a collision occurs against the piston, all the neighbouring particle's collision times need to be updated, and correspondingly shifted in the queue. If we directly updated the events from inside the heap, it would no longer be well-ordered. As such one would have to either maintain the heap structure using bubble up/down methods (using the pre-existing well-ordering of the heap, prior to updating the event), re-order the heap structure 'from scratch' (which costs $\mathcal{O}(3N)$ comparisons), or remove (or mark the old event as void) and re-insert the event into the heap, which is often $\mathcal{O}(\log N)$. The problem is made even worse that typically we do not know the index of the event in the heap array, so we need to find it first (which is either $\mathcal{O}(N)$ or $\mathcal{O}(\log N)$ depending on implementation. Because of this, we identified two different approaches and compared them.

3.3.1. A comparison between heaps and red-black trees

We remark that all algorithmic running times stated in this section can be found in [11]. First, we have the regular **binary heap** structure. It is a binary tree, where each event is a node whose key is the system time upon realizing the event. Then, one finds that every parent node's key is smaller than its children (also known as a **min**-heap). This is a relatively simple data structure that is provided in the C++ standard library through the header file `<algorithm>`. Namely it offers `make_heap` to make a heap out of an array (which is a $\mathcal{O}(n)$ process, for n the length of the array), and then `pop_heap`, `push_heap` to be used when removing (the smallest element) and inserting elements in the heap, both $\mathcal{O}(\log n)$ processes. The standard library, however, did *not* provide a method to re-position an updated node in the heap (decrease/increase-key, or in general heapify). Unfortunately, these methods generally require as input the index of the node in the array to update, but we have no way to extract that index without finding it first, which was a $\mathcal{O}(n)$ process. As such, changing the data structures and code so we could maintain the heap property was not seen as feasible due to time constraints. We resorted to simply updating the events as needed, and then calling `make_heap` to re-create the heap, incurring a $\mathcal{O}(N)$ computational cost, before returning back to Step 1.

An alternative to this was to use red-black trees. These are also binary heaps, but with the property that it is self-balancing. Unlike in the simple binary heap structure, the children of a parent node are ordered in such a way that the tree is roughly balanced, i.e. if there are $2^n - 1$ nodes in the tree, then the tree height is n. Due to this property, searches and deletions are $\mathcal{O}(\log n)$ (as they scale the depth of the tree), at the cost of an extra bit to keep track of if a node is red or black. Full details about how such a data structure is implemented can be found in [11, Ch. 13]. This data structure is also provided in the C++ standard library, using either the header files `<set>` for trees with just keys or `<map>` for trees with key, value pairs. In this case, we used the `set` structure, and for each event that needed to be updated in the queue, we would find, remove and then re-insert them into the queue, which was all $\mathcal{O}(\log N)$.

Due to the differences in implementation, the heap method performs better for small simulations (Fig 3.4a) but ultimately the $\mathcal{O}(\log N)$ scaling wins out for the red-black tree. We note that the computation times increase significantly as m_c becomes small, where in $m_c = 1$ gives the inefficient naive algorithm described in Section 3.2.1, giving us the motivation to pursue the algorithm described by [29].

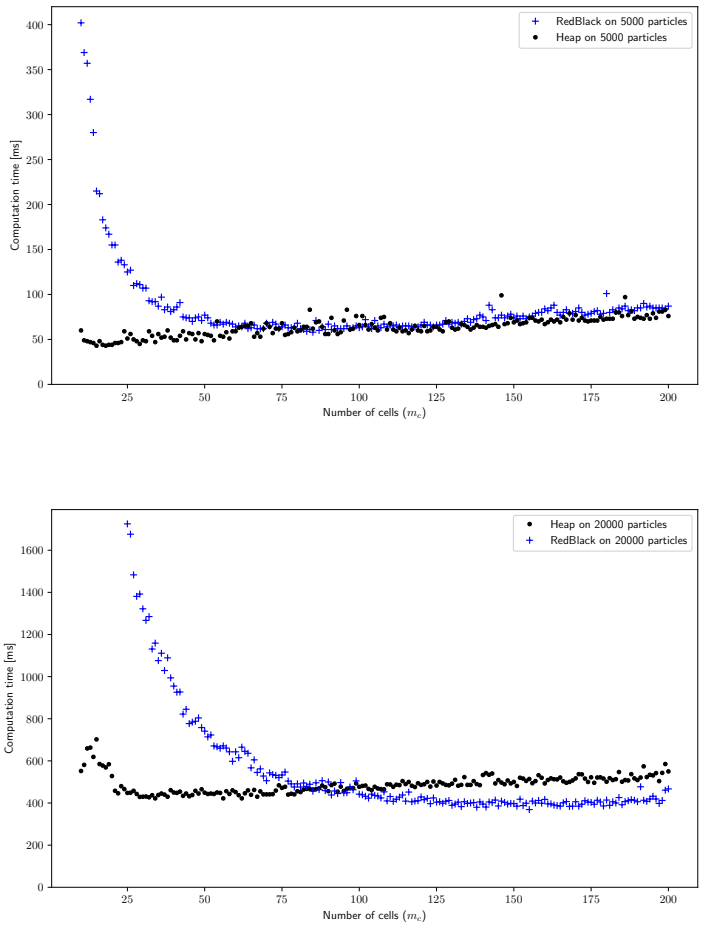

Figure 3.4: The computation times against the number of cells m_c using either a binary heap (black dot) or red-black tree (blue cross) as the event queue for (a) $N = 5000$ particles and (b) $N = 20000$ particles, simulated over a time frame $t = 5$, using the same parameters as [9]. The random number generator was seeded to ensure identical calculations were carried out between the two data structures.

Another artifact of note is the difference in the scaling of the optimum number of cells. The optimum for Figure 3.4a is for the heap structure $m_{\text{opt}} = 43$, and for the red-black structure $m_{\text{opt}} = 85$, whilst in Figure 3.4a it is $m_{\text{opt}} =, 155$ for the heap and red-black structures respectively. Unsurprisingly, the differences in the computation costs have an impact in the optimal choice for m_c, though it is surprising that the optimums for the red-black approach is *higher* than the slower heap approach. This suggests the constants associated with the $\log N$ scaling of the red-black approach are significantly larger than that of the heap approach. Nonetheless, meaningful conclusions cannot be taken from two data points (in m_{opt}) alone, and so we next sought out to optimize over the number of cells.

3.3.2. Optimizing the number of cells

As mentioned in Section 3.2.2, there is an interplay in the computational costs of determining the next collision (for particles in cells neighbouring the piston), and the costs of transferring particles between cells. As suggested in Figure 3.4, picking m_c too low or high can lead to a slower algorithm. To make this more concrete, we sought to determine m_{opt} over varying N, and how the computation time scales with N in this optimum. The former, to then use for large scale simulations where optimizing over m_c would simply take too much time, and the latter to confirm the efficiency of the algorithm.

Before we delve into the data, we must remark that computation times are quite peculiar to measure. Indeed, depending on the presence of background tasks, computer specs, power settings and if the program is running in the foreground or not, one can get wildly different results. Moreover, it does not necessarily

represent the actual CPU or processor time spent running the program. Unfortunately, measuring the CPU cycles a program uses during its runtime is practically impossible to measure, so the computation time acts as a barometer in this regard. As such, it is more worthwhile to comment on the *trends* in computation time, which persist provided the compared scenarios were run in the same environment.

We first see how the optimum number of cells m_{opt} scales with respects to N, in Figure 3.5. As we saw in

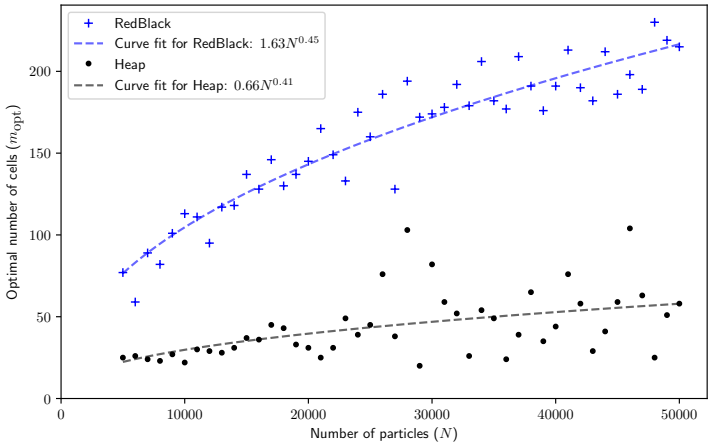

Figure 3.5: Here we find the optimum number of cells m_{opt} against N for the two data structures, for simulations up to $t = 4$ with the configuration of [9]. They were then fitted against aN^b. For the heap (black dots), we get $a = 0.7 \pm 0.8$, $b = 0.4 \pm 0.1$, and for the red-black method (blue crosses), we get $a = 1.6 \pm 0.5$, $b = 0.45 \pm 0.03$

Figure 3.4, the red-black approach has a higher m_{opt} than the heap approach. We also note that m_{opt} is very noisy for the heap approach. This is because for the heap, the computational time increase for going over m_{opt} is low (see the tail ends in Fig. 3.4). Since in [29] the computed relation is of the form $m_{\text{opt}} \sim N^b$, we then also curve-fitted the data points against the relation aN^b. As we can see in Fig. 3.5, the heap data is too noisy and level to draw any meaningful conclusions, but the red-black approach seems to have $m_{\text{opt}} \sim \sqrt{N}$.

Of interest is also the relation between the computation time and N. Since [29] predicts that the computation time scales with $\mathcal{O}(N^2 \log N)$, we initially plotted the computation time against this parameter. For the heap approach, this gives a relatively smooth linear relation (see Fig. 3.6a), with disturbances caused predominantly due to computation time randomness. However this linear fit was not observed for the red-black approach (against $N^2 \log N$ the computation time was sub-linear). Since we incur a cost of $\mathcal{O}(N)$ extra in the heap approach which becomes $\mathcal{O}(\log N)$ in the red-black approach, an alternative plot would be the red-black computation time against $N \log(N)^2$, which gives back a linear relation again (see Fig 3.6b).

Alternatively, one could also plot the computation times against $N^b \log(N)$. This was investigated in Figure 3.7. Here we can clearly see that the heap is better for low N but the red-black approach quickly be-

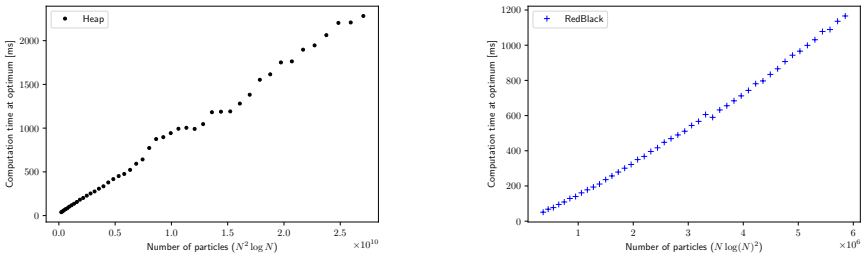

Figure 3.6: (a) The computation time for the heap approach plotted against $N^2 \log N$, which was found in [29] (albeit in a different context) indicates a relatively straight line. (b) The computation time for the red-black approach plotted against $N \log(N)^2$ also shows a straight line, and so performs better than the heap for large N. For both plots, the computation times were calculated in the same run as the m_{opt}'s in Fig. 3.5

comes better as N increases. Moreover, the curve fits of the form $aN^b \log N$ are pretty close to the data, with $a = 1.4 \pm 0.5 \cdot 10^{-7}, 7.9 \pm 0.8 \cdot 10^{-5}$ and $b = 1.95 \pm 0.03, 1.304 \pm 0.009$ for the heap and red-black approaches respectively. Unfortunately, we find that the heap approach is actually not that much better than the naive approach described in Section 3.2.1 (that scales, intuitively, with $\mathcal{O}(N^2)$).

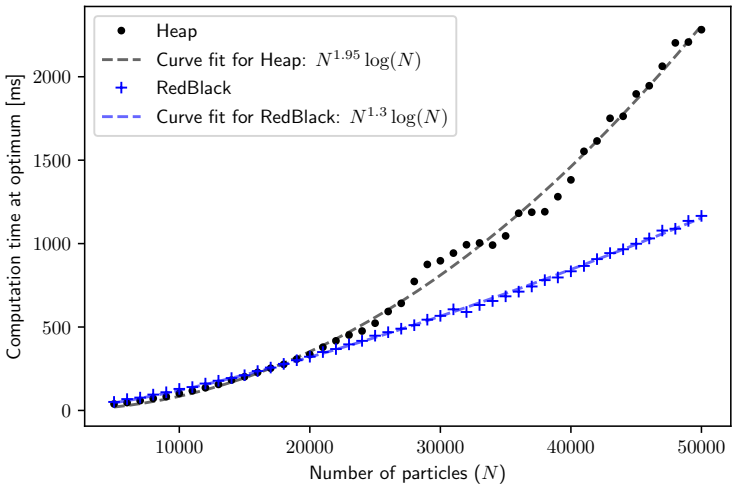

Figure 3.7: The computation time against N for m_{opt} found in Fig. 3.5, for both the heap (black dots) approach and the red-black (blue cross) approach. Both were then curve-fitted against $aN^b \log N$, where $a = 1.4 \pm 0.5 \cdot 10^{-7}, 7.9 \pm 0.8 \cdot 10^{-5}$ and $b = 1.95 \pm 0.03, 1.304 \pm 0.009$ for the heap and red-black approaches respectively.

3.4. Concluding remarks

The implementation led to two different approaches, but it is clear from Fig. 3.7 that the red-black approach is better for large N. In this approach, we have found $m_c \sim \sqrt{N}$ from Fig. 3.5. To compare, the paper that we base the algorithm on [29] found in the 1D case that $m_c \sim N$, and in general, the optimum cell sizes are such that there is on average one particle per cell. Such a result would be logical for particle-particle collisions, but too stringent for our case of only the interacting piston. So we could, heuristically, argue that the change $m_c \sim N \to \sqrt{N}$ follows from the change $N_c \sim N^2 \to N$ (with N_c being the number of collisions), though this argument proves tedious to formalize. Nonetheless, though the results in 3.7 are in agreement with the results found in [29, Figs. 8,9], we suspect that the implementation could be further refined so that it scales with $\mathcal{O}(N_c \log N) = \mathcal{O}(N \log N)$ in the non-interacting particles scenario. A rigorous derivation of this result, in the spirit of Section 3.2.3, would also be of interest, where the interplay of all the parameters can be investigated separately.

We would also like to remark the data requirements for the algorithm in Section 3.2.2. For example, in the case of $L = 300$ as was [9], with the scaling described in Section 3.1.2, around 4GBs of data was needed to store all the details of the particles. No doubt some of this can be optimized, but at that level, having an event for each particle can incur a major memory cost. Avoiding storing these events, however, incurs an additional computational cost, which at $N \sim 10^7$ is hard to ignore.

There are also a few issues with floating point numbers that normally do not affect the simulation but that may be a concern for large simulations. We noted that each event is keyed by the system time at the event's occurrence. Likewise, particles store the time since their last collision, to allow for the use of Eq. 3.1 to delay the positional updates. Towards the end of a simulation run, these times are $\approx t$. But the successive times between collisions, seems to scale with $1/N$. If one uses floats (32-bit precision), then for $N \sim 10^7$ one already that t cannot be much larger than 1 (otherwise the 7 decimal places of precision gives $t + \frac{1}{N} \approx t$, and so the event does not progress the system time.

3.4.1. Future work

Our approach treated the piston separate from the particles, and so made the piston the only particle without collision events. An alternative, would be to have the piston handle all the collision events, and the particles would simply have transfer or wall collision events. One could also improve the implementation, in particular the process of maintaining the heap after updates, with custom code to at least reduce the expensive constants incurred by finding, removing and reinserting in the red-black approach. An example of this is using the C++17 standard, which gives the method `std::set<key>.extract`. This both finds and removes the node, whose key-value can then be modified freely and then reinserted.

Another potential improvement for the optimality of the algorithm, is by making the cells non-uniform in length. In particular, for the case of a piston centered in the middle of the cylinder, that oscillates around this initial position (as in Figure 3.1), it may be better to pick cell lengths that decrease as one approaches the center. Assuming the number of cells m_c remains fixed, this should not meaningfully change the number of transfer events handled per collision, but the thinner cells around the piston could significantly reduce the number of collision events updated. Such dynamic cell shape algorithms have been explored [13, 28], but for complicated shapes lead to problems in determining which particle is in which cell (and which cells are neighbouring). We can, however, exploit the regularity of our 1 dimensional case to, for example, make the cells lengths geometric as one approaches the hard boundaries to the center.

Whilst we predominantly concerned ourselves with recreating the results of Lebowitz and Chernov's simulation [9], with eventually the optimal algorithm in Sigurgeirsson et al.'s [29], one may be interested in adjusting the degrees of freedom in the simulation given in Section 3.1.1. Some do not majorly affect the simulation (changing the mass ratio in the scaling given in Section 3.1.2, for example, only reduces the amplitude of oscillations across the board). But others are of particular interest, namely different initial distributions f_0, and periodic boundary conditions. Other parameters can be investigated over different scaling limits, too. And one could see if forcing $\langle v^2 \rangle_1 = \langle v^2 \rangle_2$ to be equal on both sides at the start may kill off any oscillation, or if the spatial component of the simulation still forces a very minor degree of oscillation.

Lastly, one can also look at collecting different types of data. Due to time constraints, we could not discuss in detail how the particle distributions evolve over time, by running an ensemble of simulations (with the same parameters, just different random realizations of f_0), which would've been of particular interest in Chapter 5. One can also look at how the macroscopic temperature of both sides evolve over time, as was done in [6, 21]. The derived relations for m_{opt}, then, allows for future simulations to be done without major concern for optimality.

4

The H-theorem and convergence to equilibrium

The H-theorem is a series of results, varying on the kinetic equation used, that implies a convergence to equilibrium. In the most general sense, there is often a functional $H(f) = \int A(f)d\vec{v}$, such that solutions to the kinetic equation give rise to $\frac{d}{dt}H(f) \leq 0$. In nice enough cases, one can find an equilibrium distribution f_∞ that minimizes H, and so in a sense one would expect $\lim_{t\to\infty} f(t,\vec{x},\vec{v}) = f_\infty(\vec{x},\vec{v})$. Thankfully, such a H-theorem has been described for the general case of the Boltzmann equation (2.9), although rigorous proofs, as like many other topics in the field, prove to be far more elusive. Given we have a sense of convergence towards equilibrium through the H-theorem, it is natural to ask what the rate of convergence is. Often times it is very difficult to show the rate of convergence, but if the rate of change of H given by the H-theorem can be bounded by H, then exponential convergence quickly follows. Fortunately, in the case of the Fokker-Planck equation found in Section 2.4, we can find the relevant H functional, the corresponding H-theorem and an exponential rate of convergence, which we will show at the end of the chapter. Unfortunately the results do not extend to our *kinetic* Fokker-Planck equation (Eq. 2.24), but a generalized convergence to equilibrium is still recovered. To start off, we will state and prove the general H-theorem.

4.1. H-theorem for the Boltzmann equation

We consider the time evolution of the functional:

$$\mathscr{H}(f) = \int_{\mathbb{R}^d}\int_{\mathbb{R}^d} f\log f\, d\vec{v}\, d\vec{x} \tag{4.1}$$

This functional is sometimes called the **Boltzmann's $\mathscr{H}$ functional**, or the **entropy functional**. Indeed, if the reader is familiar with information theory, this is equivalent to Shannon's entropy, up to the sign [30]. The time evolution of this functional is as follows:

$$\frac{d}{dt}\mathscr{H}(f) = \int \partial_t(f\log(f))\, d(\vec{v},\vec{x}) = \int \partial_t f\log(f) + f\frac{\partial_t f}{f}\, d(\vec{v},\vec{x}) = \int \partial_t f\log(f)\, d(\vec{v},\vec{x}) + \frac{d}{dt}\int f\, d(\vec{v},\vec{x})$$

For the last term in the equation, we see that this expression is the same as the rate of change of the total mass (Eq. 2.18), which is a conserved quantity for solutions of the Boltzmann equation, so it evaluates to 0. Substituting the Boltzmann equation (Eq. 2.9) in for $\partial_t f$ and using the fact that the transport term does not contribute to this functional (Lemma 2.2.2), we get:

$$\frac{d}{dt}\mathscr{H}(f) = \int_{\mathbb{R}^d}\int_{\mathbb{R}^d} Q(f,f)\log(f)\, d\vec{v}\, d\vec{x} \tag{4.2}$$

We see that this is of the form of one of the expressions in Maxwell's weak formulation. Indeed, if we symmetrize equation 2.12, by bringing it back to something of the form $\int B\cdot(f'f'_* - ff_*)\cdots d\vec{v}$, we get:

$$\int_{\mathbb{R}^d} Q(f,f)\varphi\, d\vec{v} = -\frac{1}{4}\int_{\mathbb{R}^d\times\mathbb{R}^d}\int_{\mathbb{S}^{d-1}} B(\vec{v}-\vec{v}_*,\sigma)(f'f'_* - ff_*)(\varphi'+\varphi'_*-\varphi_*-\varphi)\, d\sigma\, d(\vec{v},\vec{v}_*) \tag{4.3}$$

We see that the left-hand side of this equation is of the same form as the right-hand side of (4.2), where $\varphi = \log(f)$. Indeed, plugging this expression in, without care for regularity constraints, gives us:

$$\frac{d}{dt}\mathscr{H}(f) = -\int_{\mathbb{R}^d} D(f)\, d\vec{x}, \quad D(f) := \frac{1}{4}\int_{\mathbb{R}^d\times\mathbb{R}^d}\int_{\mathbb{S}^{d-1}} B(\vec{v}-\vec{v}_*,\sigma)(f'f'_* - ff_*)(\log(f'f'_*) - \log(ff_*))\, d\sigma\, d(\vec{v},\vec{v}_*) \tag{4.4}$$

Where $D(f)$ is the **entropy dissipation functional**. To see that $D(f) \geq 0$, we need to observe the fact that the function $(X,Y) \mapsto (X-Y)(\log(X)-\log(Y))$ is non-negative. We will prove this below:

Lemma 4.1.1. *The function $F : (\mathbb{R}_{\geq 0})^2 \to \mathbb{R}$ given by $F(x,y) = (x-y)(\log(x)-\log(y))$ is non-negative.*

Proof. We see that for $x = y$, $F(x,x) = 0$. We will prove that this is the global minimum. The partial derivatives of F are as follows:

$$\partial_x F = (\log x - \log y) + \frac{x-y}{x}, \quad \partial_y F = (\log y - \log x) + \frac{y-x}{y}$$

Any critical point must satisfy both $\partial_x F = 0$ and $\partial_y F = 0$. If we let $t = \frac{y}{x}$, we see that:

$$\begin{aligned} \partial_x F = 0 &\implies \log\left(\frac{x}{y}\right) - \frac{y}{x} + 1 = 0 &&\implies \log(t) + t = 1 \\ \partial_y F = 0 &\implies \log\left(\frac{y}{x}\right) - \frac{x}{y} + 1 = 0 &&\implies \log(t) - t^{-1} = -1 \end{aligned}$$

Subtracting the two equations from each other we get:

$$t + t^{-1} = 2 \implies t^2 - 2t + 1 = 0 \implies (t-1)^2 = 0$$

So the only critical points are at $t = 1$, i.e. $x = y$. To determine if this is then a global minimum, we must compute the Hessian. The second partial derivatives are as follows:

$$\partial_{xx}F = \frac{1}{x} + \frac{y}{x^2} = \frac{x+y}{x^2}, \quad \partial_{xy}F = -\frac{1}{x} - \frac{1}{y} = -\frac{x+y}{xy} = \partial_{yx}F, \quad \partial_{yy}F = \frac{1}{y} + \frac{x}{y^2} = \frac{x+y}{y^2}$$

Hence, the Hessian matrix is given by:

$$H_F(x,y) = (x+y)\begin{bmatrix} \frac{1}{x^2} & \frac{-1}{xy} \\ \frac{-1}{xy} & \frac{1}{y^2} \end{bmatrix} = \frac{x+y}{x^2y^2}\begin{bmatrix} y^2 & -xy \\ -xy & x^2 \end{bmatrix}$$

To determine whether or not this matrix is positive semi-definite, we will compute the eigenvalues of the re-scaled matrix, $\tilde{\lambda}_1, \tilde{\lambda}_2$. We see very clearly that the determinant $\det = y^2x^2 - (-xy)^2 = 0$, so one of the eigenvalues is $\tilde{\lambda}_1 = 0$. The associated eigenvector is $[x,y]^T$, and so we can find the associated eigenvector for the second eigenvalue by finding the perpendicular vector $[-y,x]^T$. Computing the matrix-vector product gives us $\tilde{\lambda}_2 = x^2 + y^2$. Re-scaling the eigenvalues so that they represent the eigenvalues of H_f, we get $\lambda_1 = 0, \lambda_2 = (x^2+y^2)(x+y)/x^2y^2$. Since both eigenvalues are non-negative for any $x, y \in \mathbb{R}_{\geq 0}$, we conclude that H_F is positive semi-definite. Through Taylor's theorem in 2 variables, this gives us that $F(x,x) = 0$ is the global minimum. Indeed, we get:

$$F(x,y) = F(0,0) + \nabla F(0,0)\cdot\begin{bmatrix} x \\ y \end{bmatrix} + \frac{1}{2}\begin{bmatrix} x & y \end{bmatrix} H_F(\xi_x,\xi_y)\begin{bmatrix} x \\ y \end{bmatrix} = 0 + c_1^2\lambda_1|u_1|^2 + c_2^2\lambda_2|u_2|^2 \geq 0$$

Where $[x,y]^T = c_1\vec{u}_1 + c_2\vec{u}_2$ and $\vec{u}_1, \vec{u}_2$ are an orthogonal basis of eigenvectors for $H_F(\xi_x,\xi_y)$, and $\xi_x \in (0,x), \xi_y \in (0,y)$ are unknown error terms. So we have that $F(x,y) \geq 0$ as required. □

With this result, it is clear that $D(f) = \int B \cdot F(f'f'_*, ff_*)d(\sigma,\vec{v}_*,\vec{v})$ and so is non-negative, a consequence of this is then:

Theorem 4.1.2 (Boltzmann's $\mathscr{H}$ theorem)**.** *For all solutions of the Boltzmann equation (2.9), the entropy functional $\mathscr{H}$, as given in Eq. 4.1, is non-increasing in time, i.e.:*

$$\frac{d}{dt}\mathscr{H}(f) = -\int_{\mathbb{R}^d} D(f)\, d\vec{x} \leq 0$$

Evidently, this suggests a sort of convergence to the solutions of the functional equation $D(f) = 0$, or more clearly that $f'f'_* = ff_*$ almost everywhere over the integration range $(\sigma, \vec{v}_*, \vec{v}) \in \mathbb{S}^{d-1} \times \mathbb{R}^d \times \mathbb{R}^d$. That these would give rise to an equilibrium solution of the Boltzmann equation is self-evident. If we recall the **chaos assumption** in Chapter 2, we can link ff_* to a two particle distribution $f^{(2)}$. Then, the equality $f'f'_* = ff_*$ simply assigns the same probability to a pair of particles with pre-collision velocities (v, v_*), and to a pair with post-collision velocities (v', v'_*). One can check that the Maxwellian distribution satisfies this, and hence is an equilibrium solution of the Boltzmann equation.

4.2. H-theorem for our Fokker-Planck equation

We will derive in chapter 5 that the following Fokker-Planck equation describes the time evolution of the particles:

$$\partial_t f = \nabla_v \cdot (|v|\nabla_v f + |v|\vec{v} f) \tag{4.5}$$

In comparison to the generic linear Fokker-Planck equation introduce in section 2.4, namely Equation 2.22, we find that the dissipation and friction coefficients have both been made functions of $\vec{v}$. We remark that we are dealing with a **spatially homogeneous** scenario, that is to say f no longer explicitly depends on $\vec{x}$ (it is a uniform probability density over $\vec{x}$). That is why the transport operator does not appear in Eq. 4.5.
We will now compute the time evolution of Boltzmann's $\mathscr{H}$-functional for some f that solves Eq. 4.5, and see where it goes wrong in recreating a $\mathscr{H}$-theorem result.

4.2.1. Determining the appropriate functional

We note that in Chapter 5, we will be deriving (4.5) in only one dimension $d = 1$. As such, we will proceed with our computations in 1D. We will see towards the end of this section how the argument generalizes to higher dimensions. As we computed earlier, we find that the time evolution of $\mathscr{H}$ is given by:

$$\frac{d}{dt}\mathscr{H}(f) = \int_{\mathbb{R}} \partial_t f \log f \, dv = \int_{\mathbb{R}} \partial_v \Big(|v|\partial_v f + |v| v f \Big) \log f \, dv$$

Where for the second equality we used the fact that f is a solution of (4.5). Integration by parts yields:

$$\frac{d}{dt}\mathscr{H} = \int_{-\infty}^{\infty} \partial_v \left(|v|\partial_v f + |v| v f \right) \log f \, dv = \Big[(|v|\partial_v f + |v| v f) \log f \Big]_{-\infty}^{\infty} - \int_{-\infty}^{\infty} (|v|\partial_v f + |v| v f) \partial_v (\log f) \, dv \tag{4.6}$$

We now consider the case of the boundary term. Since f is a probability distribution, we know that $\lim_{v\to\pm\infty} f(v,t) = 0$ (otherwise integrability fails). Intuitively, one would argue that as a consequence the boundary term in (4.6) goes to 0. However, we also have the issue of $\log f$ going to $-\infty$, and naturally the v terms blowing up to infinity. So we will approach this with some care. We note that there are additional integrability constraints on f.

Assumption. For f, the macroscopic properties given in Definition 2.2.1 are **finite**. In other words, the integrals $\int f \, dv, \int vf \, dv, \int |v|^2 f \, dv$ all converge and are finite.

From this integrability of $\int |v|^2 f \, dv$, we have that $\lim_{v\to\pm\infty} |fv^2| = 0$, using the fact that f is non-negative. We can now employ L'Hopital's rule, on $\alpha = f|v|^2$. Indeed, we know as $v \to \pm\infty$, $\alpha \to 0$. We observe:

$$\lim_{\alpha\to 0} \alpha \log \alpha = \lim_{\alpha\to 0} \frac{\log \alpha}{1/\alpha} = \lim_{\alpha\to 0} \frac{1/\alpha}{-1/\alpha^2} = \lim_{\alpha\to 0} -\alpha = 0$$

Hence we have shown $|v|^2 f \log\big(|v|^2 f\big) \to 0$ as $|v| \to \infty$. However, in this limiting regime, we certainly have $|v|^2 \geq 1$ so $\log\big(|v|^2\big) \geq 0$ and so we can say

$$\forall |v| \geq 1 : \qquad f \log f \leq |v|^2 f \log f \leq |v|^2 f \left(\log f + \log |v|^2 \right) = |v|^2 f \log\big(f|v|^2\big)$$

Since we have both sides converging to 0 as $|v| \to \infty$, we conclude $|v|^2 f \log f \to 0$ by the Squeeze Lemma. The $|v|(\partial_v f)\log f$ term converges faster to 0, as $|v|\partial_v f$ is integrable in the same order as f. Indeed, see:

$$\begin{aligned} \int_{-\infty}^{\infty} |v|\partial_v f \, dv &= \int_0^{\infty} v\partial_v f \, dv + \int_{-\infty}^{0} -v\partial_v f \, dv \\ &= \big[vf \big]_0^{\infty} + \big[-vf \big]_{-\infty}^{0} - \int_0^{\infty} f \, dv + \int_{-\infty}^{0} f \, dv \end{aligned}$$

The boundary term vanishes by the integrability of $\int v f\, dv$, and so we find we can bound $\int |v|\partial_v f\, dv$ both above and below by $\pm\int_{-\infty}^{\infty} f\, dv$, which is again finite.
So we have shown that the boundary term in (4.6) vanishes, and the remaining integral gives:

$$\frac{d}{dt}\mathscr{H} = -\int_{-\infty}^{\infty} \left(|v|\partial_v f + |v| v f\right)\partial_v(\log f)\, dv = -\int_{-\infty}^{\infty} \left(|v|\partial_v f + |v| v f\right)\frac{1}{f}\partial_v f\, dv = -\int_{-\infty}^{\infty} |v|(\partial_v f)^2 + |v| v \partial_v f\, dv$$

Now we see how $\frac{d}{dt}\mathscr{H} \leq 0$ need not hold, due to the $-\int |v| v \partial_v f\, dv$ term. Indeed, if v and $\partial_v f$ have opposite signs then the integral is negative, and thus its contribution to $\frac{d}{dt}\mathscr{H}$ is positive. This suggests that we should cancel out this $|v| v \partial_v f$ term in some way by adding a term to the functional. Since the functional undergoes an integration by parts, it would be illustrative to guess something of the form $f \cdot g(v)$.
So now let us consider the functional

$$H(f) = \int_{-\infty}^{\infty} f \log f + f g(v)\, dv \tag{4.7}$$

We can reuse our earlier computations to find:

$$\frac{d}{dt}H(f) = \int \partial_t f \log f + \partial_t f g(v)\, dv$$

Substituting the kinetic Fokker-Planck equation (4.5) and applying integration by parts as before (assuming the g term does not cause a non-zero boundary term), we get:

$$\frac{d}{dt}H(f) \quad = \quad -\int_{-\infty}^{\infty} \left(|v|\partial_v f + |v| v f\right)\left(\frac{1}{f}\partial_v f + g'(v)\right) dv \quad = \quad -\int_{-\infty}^{\infty} \frac{|v|}{f}\left(\partial_v f + v f\right)\left(\partial_v f + g'(v) f\right) dv \tag{4.8}$$

A natural choice for g would be such that it solves $g'(v) = v$, namely $g(v) = v^2/2$. Then the two bracketed terms at the end of the equation are identical, and thus we get:

$$\frac{d}{dt}\int_{-\infty}^{\infty} f \log f + f \cdot v^2/2\, dv = -\int_{-\infty}^{\infty} \frac{|v|}{f}\left(\partial_v f + v f\right)^2 dv \tag{4.9}$$

The term in the integral is clearly non-negative, and so we find that $\frac{d}{dt}H(f) \leq 0$.
The generalization to higher dimensions is achieved by replacing regular integration by parts with the product rule for the divergence operator, namely: $\nabla \cdot (g\vec{F}) = (\nabla \cdot \vec{F})g + \nabla g \cdot \vec{F}$. Following the same steps, one finds that the extra term g in the H functional (see equation 4.7) must satisfy $\nabla g = \vec{v}$ which suggests $g = |\vec{v}|^2/2$. To summarize, we have shown the following:

Theorem 4.2.1 (H-theorem for Eq. 4.5)**.** *For solutions of (4.5), the functional:*

$$H(f) = \int_{\mathbb{R}^d} f \log f + f\frac{|\vec{v}|^2}{2}\, d\vec{v} \tag{4.10}$$

satisfies the H-theorem, with the entropy dissipation $D(f)$ given by:

$$\frac{d}{dt}H(f) = -D(f) := -\int_{\mathbb{R}^d} \frac{|\vec{v}|}{f}\left|\nabla_v f + \vec{v} f\right|^2 d\vec{v} \tag{4.11}$$

The functional (4.10) we have found is known as the **free energy** [30, pg. 108] of the system, or the relative Maxwell-Boltzmann entropy (for the Fokker-Planck equation).

4.3. Convergence to equilibrium

Whilst the H-theorem(s) imply a convergence to an equilibrium, it is often a more difficult process to quantify the rate of this convergence. Nonetheless, in introducing the Boltzmann collision kernel and $\mathscr{H}$-theorem, Boltzmann showed convergence towards a Maxwellian distribution [3]. As such, it is of greater interest to see if the rate of convergence can be proven, or at the very least bounded.

4.3.1. General approaches

One of the easiest approaches to show a convergence to equilibrium is through Grönwall's Lemma. We will restate it below:

Lemma 4.3.1 (Grönwall's Lemma)**.** *We present the lemma in its differential form. Let $I \subset \mathbb{R}$ be a non-empty interval, $t_0 \in I$ and $u, v : I \to \mathbb{R}$ be continuous. If we have:*

$$\forall t \in I, t \geq t_0 : \quad u'(t) \leq v(t)u(t)$$

Then u is bounded by the solution of the corresponding differential equation $u' = vu$, i.e.:

$$\forall t \in I, t \geq t_0 : \quad u(t) \leq u(t_0) \cdot e^{\int_{t_0}^{t} v(s)ds}$$

Proof. Let $w(t) = \exp\left(\int_{t_0}^{t} v(s)ds\right)$. We have, by the quotient rule:

$$\frac{d}{dt}\frac{u(t)}{w(t)} = \frac{u'(t)w(t) - w'(t)u(t)}{w(t)^2} = \frac{u'(t)w(t) - v(t)w(t)u(t)}{w(t)^2} = \frac{1}{w(t)}\Big(u'(t) - v(t)u(t)\Big)$$

Now $w(t) > 0$ for all times $t \geq t_0$, and since $u' < vu$, we conclude $\frac{d}{dt}\frac{u}{w} \leq 0$. So the derivative of the function u/w is non-positive, and the function is therefore decreasing for $t \geq t_0$. Therefore, it obtains its maximum at $t = t_0$, so we have:

$$\frac{u(t)}{w(t)} \leq \frac{u(t_0)}{w(t_0)} = u(t_0) \implies u(t) \leq u(t_0)w(t) = u(t_0) \cdot e^{\int_{t_0}^{t} v(s)ds}$$

□

If one can acquire a bound on $\frac{d}{dt}H(f)$ in terms of $H(f)$, then Grönwell's Lemma gives a direct pathway to determining the rate of convergence. Indeed, suppose we had a bound of the form:

$$\lambda H(f(t,\cdot)) \leq D(f(t,\cdot)), \quad \lambda > 0. \tag{4.12}$$

Then noting that $\frac{d}{dt}H(f) = -D(f)$, we get:

$$\frac{d}{dt}H(f) \leq -\lambda H(f) \implies H(f(t,\cdot)) \leq H(f(0,\cdot))e^{-\lambda t}$$

How does this then prove convergence? Depending on the functional and equation, one can link $H(f)$ to the 'distance' between the function and the equilibrium distribution (and in the special case, the real *distance*, as we will see in Section 4.3.2). Let us take, as an example, the original $\mathscr{H}$ functional (Eq. 4.1). If $\rho, \vec{u}, T$ are all defined by the formulas given in Definition 2.2.1, and we are dealing with the spatially homogeneous case (this makes the macroscopic observable constant), then it is clear that the equilibrium solution to the Boltzmann equation (2.9) is given by [30, pg. 107]:

$$M^f(\vec{v}) = \frac{\rho}{(2\pi T)^{d/2}} e^{-\frac{|\vec{v}-\vec{u}|^2}{2T}} \tag{4.13}$$

Since M^f and f share the same moments up to order 2, we can rewrite $\mathscr{H}(f)$ in terms of something known as the **Kullback relative entropy** of f with respect to M^f.

Lemma 4.3.2. *For a solution f of the Boltzmann equation (2.9) in the spatially homogeneous setting, and for $\mathscr{H}$ given by (4.1), M^f given by (4.13), we have:*

$$\mathscr{H}(f) - \mathscr{H}(M^f) = \int_{\mathbb{R}^d} f \log \frac{f}{M^f}\, d\vec{v} =: \mathscr{H}(f|M^f) \tag{4.14}$$

Proof. The crux is an algebraic trick, made possible by the fact that f and M^f share the same moments up to order 2. That is to say:

$$\int_{\mathbb{R}^d} f\, d\vec{v} = \int_{\mathbb{R}^d} M^f\, d\vec{v}, \quad \int_{\mathbb{R}^d} \vec{v} f\, d\vec{v} = \int_{\mathbb{R}^d} \vec{v} M^f\, d\vec{v}, \quad \int_{\mathbb{R}^d} |v|^2 f\, d\vec{v} = \int_{\mathbb{R}^d} |v|^2 M^f\, d\vec{v}.$$

That this holds is unsurprising given the definition of M^f. Nonetheless, starting from the left hand side of (4.14) we have:

$$\mathscr{H}(f) - \mathscr{H}(M^f) = \int_{\mathbb{R}^d} f\log f - M_f \log M_f \, d\vec{v}$$

We would like to add a $\int (M^f - f)\log M^f$ term, so that we can recover $\int f\log f - f\log M^f$ giving us the right hand side of (4.14). Thankfully, this is the same as adding zero. See:

$$\begin{aligned}\int_{\mathbb{R}^d} (M^f - f)\log M^f \, d\vec{v} &= \int_{\mathbb{R}^d} (M^f - f)\left(-\frac{|\vec{v}-\vec{u}|^2}{2T} - \frac{d}{2}\log(2\pi T) + \log\rho\right) d\vec{v} \\ &= \int_{\mathbb{R}^d} (M^f - f)\left(-\frac{|v|^2}{2T} + \frac{\vec{v}\cdot\vec{u}}{T} - \frac{|u|^2}{2T} - \frac{d}{2}\log(2\pi T) + \log\rho\right) d\vec{v}\end{aligned}$$

Again, since $\rho, \vec{u}, T$ are constants, and the moments are equal for M^f and f, the integral evaluates to 0. So:

$$\mathscr{H}(f) - \mathscr{H}(M^f) = \int_{\mathbb{R}^d} f\log f - M^f \log M^f + (M^f - f)\log M^f \, d\vec{v} = \int \mathbb{R}^d f\log f - f\log M^f \, d\vec{v} = \int_{\mathbb{R}^d} f\log\frac{f}{M^f}\, d\vec{v}$$

□

What is nice about this result, is that the Boltzmann H-theorem, Theorem 4.1.2, still applies for the relative entropy $\mathscr{H}(f|M^f)$. Moreover, we can show that $\mathscr{H}(f|M^f) \geq 0$ as f and M^f have the same mass ρ. Indeed, from the inequality $\log x \leq x - 1$ one can then acquire $\mathscr{H}(f|M^f) \geq \int M_f - f = 0$

Lemma 4.3.3 (Gibb's Lemma)**.** *For the relative entropy one has $\mathscr{H}(f|M^f) \geq 0$ with equality if and only if $f = M^f$.*

Proof. The proof follows from the inequality $\log x \leq x - 1$. If we let $\phi(x) = x - 1 - \log(x)$, then it has a clear root at $x = 1$. Taking derivatives, we see $\phi'(x) = 1 - \frac{1}{x}, \phi''(x) = \frac{1}{x^2}$. We see that $\phi'(1) = 0, \phi''(x) > 0$ so we conclude that $x = 1$ is a global minimum. Moreover, it is the *only* solution of $\phi'(x) = 0$, so it is the *unique* global minimum. Applying this on the relative entropy, we have:

$$\mathscr{H}(f|M^f) = \int_{\mathbb{R}^d} f\log\frac{f}{M^f}\, d\vec{v} = \int_{\mathbb{R}^d} f\left(-\log\frac{M^f}{f}\right) d\vec{v} \geq \int_{\mathbb{R}^0} f\left(1 - \frac{M^f}{f}\right) d\vec{v}$$

Expanding the last integral, and noting f and M^f have the same mass ρ, gives us the desired inequality. Equality holds again if $M^f/f = 1$, giving us the desired statement. □

Hence, through Gibb's Lemma and Boltzmann's $\mathscr{H}$-theorem, we get a generalized convergence to equilibrium. $\mathscr{H}[f|M^f]$ is decreasing and bounded from below, and only achieves its lower bound when $f = M^f$, as expected. We can analogously derive this generalized convergence result for our H-functional (4.10) and kinetic Fokker-Planck equation (4.5), by noting that the H-function is *already* in the form of a Kullback relative entropy functional. Indeed, we have:

$$H(f) = \int_{\mathbb{R}^d} f\log f + f\frac{|\vec{v}|^2}{2}\, d\vec{v} = \int_{\mathbb{R}^d} f\left(\log f - \log\left(e^{-\frac{|\vec{v}|^2}{2}}\right)\right) d\vec{v} = \int_{\mathbb{R}^d} f\log\left(\frac{f}{e^{-|\vec{v}|^2/2}}\right) d\vec{v} = \mathscr{H}(f|M)$$

Although $M = e^{-|\vec{v}|^2/2}$ doesn't have the same mass as f, one can bound $H(f)$ from below again through the fact:

$$H(f) = \int_{\mathbb{R}^d} f\log\left(\frac{f}{Ce^{-|\vec{v}|^2/2}}\right) + f\log C\, d\vec{v} = \mathscr{H}(f|Ce^{-|\vec{v}|^2/2}) + \rho\log C$$

For any constant C (and so in particular for the normalization constant that gives the same mass).

4.3.2. Rates for the Fokker-Planck equation

Although the result of convergence to equilibrium is nice for both the generic Boltzmann case and our specific kinetic Fokker-Planck equation (4.5), one may wonder what the rate of convergence is. As we mentioned before, Grönwall's Lemma is an excellent tool for this, provided a bound can be found of the form (4.12). Fortunately, in the case of the linear Fokker-Planck equation (2.22), we can find such a bound.
We will be working with the general equation:

$$\partial_t f = \nabla_v \cdot (\nabla_v f + \alpha\vec{v} f) \tag{4.15}$$

Which is of the same form as (2.22), up to a constant. As outlined in Eq. (2.23), we have that the equilibrium solution is proportional to $e^{-\alpha|v|^2/2}$. For this equation, the natural functional for a H-theorem is (4.10), and from the same analysis we have performed earlier in Section 4.2.1, we can conclude $H(f) \geq 0$ for solutions of the Fokker-Planck equation above. We will now state, without proof, the crucial bound we need:

Theorem 4.3.4 (Stam-Gross logarithmic Sobolev inequality)**.** *For any probability distribution f (absolutely continuous with respects to $e^{-|v|^2/2}$), one has:*

$$2\mathscr{H}(f|M) \leq I(f|M)$$

Where $M = (2\pi)^{-d/2}e^{-|v|^2/2}$ is the standardized Maxwellian distribution, $\mathscr{H}(f|g)$ is the (Kullback) relative entropy (4.14), and $I(f|M) := \int f|\nabla_v(\log f/M)|^2 = \int |\nabla_v f + vf|^2/f$ is known often as the (relative) Fisher information.

We note that $I(f|M)$ is almost identical to the form of $D(f)$ given by (4.11), which has an extra $|v|$ term. By a simple rescaling then, if M_σ is a Maxwellian distribution with variance σ, we have: [22]

$$\frac{2}{\sigma}\mathscr{H}(f|M_\sigma) \leq D(f) \tag{4.16}$$

From this and the framework we set out in Section 4.3.1, we can derive that $\mathscr{H}(f|M)$ decays exponentially in time. However, this result is made even stronger by the following inequality:

Theorem 4.3.5 (Csiszár-Kullback inequality)**.** *Let f, g be non-negative functions in $L^1(\mathbb{R}^d)$ with $\|f\|_1 = \int_{\mathbb{R}^d}|f| = 1$, and $\|g\|_1 = 1$. Then we have:*

$$\|f-g\|_1^2 \leq 2\mathscr{H}(f|g)$$

Where $\mathscr{H}(f|g) = \int_{\mathbb{R}^d} f\log\frac{f}{g}$ is the (Kullback) relative entropy. [16, Thm. 3]

To prove this, we need to use the following property of the function $\Phi(x) := x\log x - x + 1$.

Lemma 4.3.6. *It holds that:*

$$\Phi(x) := x\log x - x + 1 \geq \frac{3(x-1)^2}{2(x+2)} =: F(x), \qquad \forall x \geq 0 \tag{4.17}$$

Proof. Taking first and second derivatives on both sides gives $\Phi'(x) = \log x, \Phi''(x) = 1/x$ and for the other function F we have:

$$F(x) = \frac{3(x+2-1)^2}{2(x+2)} = \frac{3}{2}\left(x+2-3+\frac{9}{x+2}\right) = \frac{3}{2}(x-1) + \frac{27}{2(x+2)}$$

Hence: $F'(x) = \frac{3}{2} - \frac{27}{2(x+2)^2}$ and $F''(x) = \frac{27}{(x+2)^3}$. If we show the inequality:

$$\Phi''(x) = \frac{1}{x} \geq \frac{27}{(x+2)^3} = F''(x)$$

holds, we can integrate twice to recover our desired inequality. In other words, we must show $(x+2)^3 \geq 27x$, or equivalently $x^3 + 6x^2 - 13x + 8 \geq 0$. This has the obvious root at $x = 1$, and we find the first derivative $3x^2 + 12x - 13$ (which is greater than 0 at $x = 1$) and second derivative $6x + 12 \geq 0$ for all non-negative x. Since this inequality holds, the inequality $\Phi'' \geq F''$ holds and we recover $\Phi \geq F$ as desired. □

Proof of Theorem 4.3.5. Letting $\Phi(x) = x\log x - x + 1$, we have:

$$\int_{\mathbb{R}^d}\Phi\left(\frac{f}{g}\right)g = \int_{\mathbb{R}^d} f\log\frac{f}{g} - f + 1 = \mathscr{H}(f|g) - \|f\|_1 + 1 = \mathscr{H}(f|g)$$

Where we used the fact that f has norm 1 and f, g are non-negative. Then we have:

$$\begin{aligned}\|f-g\|_1^2 &= \left(\int_{\mathbb{R}^d}|f-g|\right)^2 = \left(\int_{\mathbb{R}^d}\left|\frac{f}{g}-1\right|g\right)^2 \\ &= \left(\int_{\mathbb{R}^d}\left[|f/g-1|\frac{\sqrt{g}}{\sqrt{f/g+2}}\right]\left[\sqrt{(f/g+2)g}\right]\right)^2 \leq \left[\int_{\mathbb{R}^d}\frac{(f/g-1)^2}{f/g+2}g\right]\cdot\left[\int_{\mathbb{R}^d}\left(\frac{f}{g}+2\right)g\right]\end{aligned}$$

Where the inequality follows through Cauchy-Schwarz on the square-bracketed terms. (The expressions in the square roots are well defined, as g non-negative). Expanding the right most integral gives $\int f + 2g = \|f\|_1 + 2\|g\|_1 = 3$ and hence we have:

$$\|f-g\|_1^2 \leq 3\int_{\mathbb{R}^d} \frac{(f/g-1)^2}{f/g+2} g \leq 2\int_{\mathbb{R}^d} \Phi(f/g)g = 2\mathscr{H}(f|g)$$

Where we identify the middle inequality corresponding to Lemma 4.17. □

Taken all together, the results from both Theorems 4.3.4 and 4.3.5, combined with our previous analysis in Section 4.3.1, gives us an exponential convergence. Recalling that the equilibrium distribution for the Fokker-Planck equation (4.15) is the Maxwellian distribution with variance $\frac{1}{\alpha}$, i.e. $M_{1/\alpha}$, we get:

$$\frac{d}{dt}\mathscr{H}(f|M_{1/\alpha}) = -D(f) \overset{(4.16)}{\leq} -2\alpha\mathscr{H}(f|M_{1/\alpha})$$

By Grönwall's lemma and the Csiszár-Kullback inequality we get:

$$\|f(t,\cdot) - M_{1/\alpha}\|_1^2 \leq 2H(f(t,\cdot)|M_{1/\alpha}) \leq 2e^{-2\alpha t}\mathscr{H}(f(0,\cdot)|M_{1/\alpha}) = e^{-2\alpha t}\|f(0,\cdot) - M_{1/\alpha}\|^2$$

Hence we have strong convergence under the L^1 norm, with an exponential rate of $-\alpha$.

4.4. Closing remarks

We note that one can find stronger generalized convergence results for Fokker-Planck equations with a confining potential [1, 22]. However, in our case (4.5) is not generated by a potential, as it has an extra $|v|$ term. This throws a wrench in the machinery outlined in the above section, as this extra $|v|$ term appears in the entropy dissipation functional $D(f)$ (given by Eq. (4.11)). Nonetheless, we still managed to successfully prove convergence to equilibrium by means of bounding $H(f)$. One may note that a lot of the terminology used in this chapter has its roots in information theory, and indeed that is the case. For example, theorems 4.3.5 and in particular 4.3.4 follows from results deep in information theory and this link comes (in part) from the similarity in thermodynamic entropy, and information entropy in encoding theory. In fact, many initial results on entropy in information theory were inspired (though not always derived from) physics' entropy.

5

Derivation of Fokker-Planck equation for piston paradox

In order to derive the kinetic Fokker-Planck (Eq. 4.5) equation described in Chapter 4, we will start with a kinetic theory approach, using the Boltzmann collision operator as given in Section 2.3, and then seeing how the equation develops in the limiting case as the piston mass blows up to infinity (relative to the particle mass), and a time-scaling known as the **grazing collision limit**. To this end, however, many assumptions have to be made. Furthermore, this derivation will be *formal*, in which we will not concern ourselves with regularity conditions nor a mathematically rigorous derivation (which would prove exceedingly difficult!). Indeed, although it is known that Fokker-Planck type equations can be recovered from the Boltzmann equation through the grazing limit, the formal proof has been done only in the spatially homogeneous setting with smoothness constraints on the collision kernel B [2] [30, pgs. 98-101]. With this in mind, let us introduce the setup.

5.1. Modelling framework

We consider the **one dimensional** adiabatic piston problem. We are dealing with a flat torus, which gives rise to periodic boundary conditions, and a spatially homogeneous setting. We have a heavy piston and many identical, non-interacting particles. The particles and piston interact through elastic collisions, and the particles do *not* collide with each other. The mass of the piston is $m_p = \frac{1}{\epsilon}$, and the mass of the particles is fixed at $m = 1$. We will tag a particle, and follow how its velocity develops over time by describing the probability density function $f_\epsilon(t, v)$. As in Chapter 2, we note that $f_\epsilon(t, v)dv$ denotes the probability of finding the tagged particle with a speed between v and $v + dv$ at time t. Our goal is to then derive how $f_\epsilon(t, v)$ evolves over time. To facilitate this, we make a few assumptions.

Assumption 1 (Maxwellian Piston)**.** The piston is already in an equilibrium state, and each time the tagged particle hits the piston it is in the same 'fresh' Maxwellian state (effectively negating previous collisions). That is to say, the velocity distribution for the piston velocity, v_p, can be described by a Maxwellian distribution:

$$\mathcal{M}(v_p) = \frac{1}{\sqrt{2\pi\epsilon}} e^{-\frac{v_p^2}{2\epsilon}}$$

Whilst this is a strong assumption, we will eventually make the masses of the particles relative to the piston extremely small, and so the assumption seems well-founded for this limit. The specific form of $\mathcal{M}$ is also with this limit in mind.

Assumption 2 (Elastic collisions)**.** As described earlier, the piston and tagged particle interact by **elastic collisions**. Their post-collision velocities can be easily computed to be:

$$v_p' = v_p + \frac{2\epsilon}{1+\epsilon}(v - v_p) \tag{5.1}$$

$$v' = v + \frac{2}{1+\epsilon}(v_p - v) \tag{5.2}$$

To describe how the particles interact, however, we need another assumption, namely.

Assumption 3 (Hard spheres)**.** The particles and piston can be modelled as hard spheres. From our derivation in Section 2.3, we see that a consequence of this assumption is that the Boltzmann collision kernel is given by:

$$B(|v - v_p|, \cos\theta) = |v - v_p|$$

Wherein we used the fact that we are in 1D space to remove the dependency of $\cos\theta$ entirely, see Eq. 2.21 ($\sigma \in \mathbb{S}^0$ gives $\sigma = \pm 1$)

Assumption 4 (Symmetry)**.** Due to the periodic nature of the torus with which this model takes place in spatially, we will assume that the probability density function f_ϵ is symmetrical in v, i.e:

$$\forall t: \quad f_\epsilon(t, v) = f_\epsilon(t, -v)$$

Lastly, we want to know how the system acts in the limit $\epsilon \to 0$. We introduce for this two variables. We have first the substitution:

$$v_p = \sqrt{\epsilon}\omega \tag{5.3}$$

Motivated by Assumption **1**, since we have $v_p \sim \sqrt{\epsilon}$, this substitution ensures that ω is standard normally distributed. It also gives rise to the following expression for ω' (corresponding to v_p')

$$\omega' = \omega + \frac{2\sqrt{\epsilon}}{(1+\epsilon)}(v - \sqrt{\epsilon}\omega) \tag{5.4}$$

Time is made dimensionless through the substitution

$$\tau = 2\epsilon t \tag{5.5}$$

The combination of a substitution like (5.5) and $\epsilon \to 0$ is known as the **collision grazing limit**. With these assumptions in mind, we will formally derive the Fokker-Planck equation.

5.2. Derivation

We note that the expressions of (5.1), (5.2) are derived from the conservation of kinetic energy and momentum. Since we are interested in the limiting case of $\epsilon \to 0$, we will linearize equations (5.4) and (5.2). In the case of ω', it is easy to see that we have:

$$\omega' = \omega + 2\sqrt{\epsilon}(v - \sqrt{\epsilon}\omega) + \mathcal{O}(\epsilon^{3/2}) \tag{5.6}$$

Indeed, expanding $\frac{2\epsilon}{1+\epsilon}$ in terms of orders of ϵ gives:

$$\frac{2\epsilon}{1+\epsilon} = 2\epsilon - 2\epsilon^2 + 2\epsilon^3 \pm \ldots = 2\epsilon \sum_{n=0}^{\infty} (-\epsilon)^n$$

As expected. For v' the situation is a little more involved. From (5.2), applying the substitution (5.3), we can recover a linear term through algebraic manipulations:

$$v' = v + \frac{2}{1+\epsilon}(\sqrt{\epsilon}\omega - v) = v + \frac{2+2\epsilon-2\epsilon}{1+\epsilon}(\sqrt{\epsilon}\omega - v) = v + 2(\sqrt{\epsilon}\omega - v) - \frac{2\epsilon}{1+\epsilon}(\sqrt{\epsilon}\omega - v)$$

This gives us:

$$v' = -v + 2\sqrt{\epsilon}\omega + 2\epsilon v + \mathcal{O}(\epsilon^{3/2}) \tag{5.7}$$

These approximation terms will allow us to compute a Taylor expansion on the kinetic equation.

5.2.1. Taylor expanding the kinetic equation

Since the only collisions occurring in the modelling framework outlined in Section 5.1 are between the particle and the piston, it is reasonable to assume that the Boltzmann operator (Eq. 2.8) will be linear in f_ϵ, with $f_* \to \mathcal{M}$. In fact, these sort of linear Boltzmann equations where f_* taking the shape of a known distribution

appear frequently in kinetic theory applications [30, pg. 17]. From the spatial homogeneity and Assumption **3**, on hard spheres, we find that the kinetic equation takes the form:

$$\partial_t f_\epsilon = \int_{\mathbb{R}} |v - v_p| \Big[f_\epsilon(v') \mathscr{M}(v_p') - f_\epsilon(v) \mathscr{M}(v_p) \Big] \, dv_p$$

Applying the substitution $v_p = \sqrt{\epsilon}\omega$ gives $dv_p = \sqrt{\epsilon} \cdot d\omega$, but this $\sqrt{\epsilon}$ term is cancelled by the Maxwellian $\mathscr{M}$ function. Indeed:

$$\mathscr{M}(v_p) = \frac{1}{\sqrt{2\pi\epsilon}} e^{-v_p^2/2\epsilon} = \frac{1}{\sqrt{\epsilon}} \cdot \frac{1}{\sqrt{2\pi}} e^{-\omega^2/2} =: \frac{1}{\sqrt{\epsilon}} \cdot \mathscr{M}(\omega)$$

So we will abuse notation and refer to $\mathscr{M}(\omega)$ as the standard Gaussian distribution, even though it is derived from $\mathscr{M}(v_p)$ which has an extra $\epsilon^{-1/2}$ factor. The crucial takeaway is that the net effect of the substitution (5.3) in terms of ϵ terms is none. Under this substitution, the kinetic equation takes the form:

$$\partial_t f_\epsilon = \int_{\mathbb{R}} |v - \sqrt{\epsilon}\omega| \Big[f_\epsilon(v') \mathscr{M}(\omega') - f_\epsilon(v) \mathscr{M}(\omega) \Big] \, d\omega \tag{5.8}$$

We will now seek to expand the terms in the square brackets in increasing orders of ϵ through a Taylor expansion. That this is permissible is motivated by the form of v', ω' found in (5.7) and (5.6), we see that $-v' - v = \mathscr{O}(\epsilon^{1/2}) = \omega' - \omega$, and so we will treat these terms as the 'deviation' term in the Taylor expansion (even though they are self-referential, that is to say, $\omega' - \omega = f(\omega)$). The expansion of $\mathscr{M}$ is easy to compute and its first terms read:

$$\mathscr{M}(\omega') = \mathscr{M}(\omega) + 2\sqrt{\epsilon}(v - \sqrt{\epsilon}\omega)\mathscr{M}'(\omega) + 2\epsilon(v - \sqrt{\epsilon}\omega)^2 \mathscr{M}''(\omega) + \mathscr{O}(\epsilon^{3/2})$$

The expansion of f_ϵ is not immediately obvious. To this end we need to use Assumption **4** to apply an algebraic trick:

$$f_\epsilon(v') = f_\epsilon(-v') = f_\epsilon(v - 2\sqrt{\epsilon}(\omega + \sqrt{\epsilon}v))$$

Then the expansion is easy to compute:

$$f_\epsilon(v') = f_\epsilon(v) - 2\sqrt{\epsilon}(\omega + \sqrt{\epsilon}v)\partial_v f_\epsilon(v) + 2\epsilon(\omega + \sqrt{\epsilon}v)^2 \partial_{vv} f_\epsilon(v) + \mathscr{O}(\epsilon^{3/2})$$

With these expansions, we can find an approximation of the product. To simplify notation, we will omit the points of evaluation for $f_\epsilon, \mathscr{M}$ and their derivatives, and denote $\partial_v f_\epsilon$ as f_ϵ' (not to be confused with f', the post-collision distribution term that appeared often in Chapter 2). We have:

$$\begin{aligned}
f_\epsilon(v')\mathscr{M}(\omega') = {} & f_\epsilon(v)\mathscr{M}(\omega) \\
& + 2\sqrt{\epsilon}\Big[(v - \sqrt{\epsilon}\omega) f_\epsilon \mathscr{M}' - (\omega + \sqrt{\epsilon}v) f_\epsilon' \mathscr{M} \Big] \\
& + 2\epsilon \Big[(v - \sqrt{\epsilon}\omega)^2 f_\epsilon \mathscr{M}'' - 2(v - \sqrt{\epsilon}\omega)(\omega + \sqrt{\epsilon}v) f_\epsilon' \mathscr{M}' + (\omega + \sqrt{\epsilon}v)^2 f_\epsilon'' \mathscr{M} \Big] \\
& + 4\epsilon^{3/2} \Big[-(v - \sqrt{\epsilon}\omega)^2 (\omega + \sqrt{\epsilon}v) f_\epsilon' \mathscr{M}'' + (v - \sqrt{\epsilon}\omega)(\omega + \sqrt{\epsilon}v)^2 f_\epsilon'' \mathscr{M}' \Big] + \mathscr{O}(\epsilon^{3/2})
\end{aligned}$$

We expand the round bracketed terms and disregard the high orders of ϵ. Moreover, we will use the fact that $\mathscr{M}(\omega) \propto e^{-\omega^2/2}$. Evidently, we have $\mathscr{M}' = -\omega\mathscr{M}$ and consequently $\mathscr{M}'' = (\omega^2 - 1)\mathscr{M}$. This gives us:

$$\begin{aligned}
f_\epsilon(v')\mathscr{M}(\omega') = {} & f_\epsilon(v)\mathscr{M}(\omega) \\
& + 2\sqrt{\epsilon}\Big[-v\omega f_\epsilon - \omega f_\epsilon' \Big]\mathscr{M} && (5.9) \\
& + 2\epsilon \Big[v^2(\omega^2 - 1) f_\epsilon + 2v\omega^2 f_\epsilon' + \omega^2 f_\epsilon'' + \omega^2 f_\epsilon - v f_\epsilon' \Big]\mathscr{M} + \mathscr{O}(\epsilon^{3/2}) && (5.10)
\end{aligned}$$

It is clear that the first term will cancel out when we substitute this expansion into the kinetic equation (5.8). We will compute the action of the integral $\int |v - \sqrt{\epsilon}\omega| \circ d\omega$ for the terms (5.9) and (5.10) separately. Before we do so, we will make one last remark.

Assumption. Since the piston travels at the velocity $v_p = \sqrt{\epsilon}\omega$ and we will be taking the limit $\epsilon \to 0$, we find that the absolute difference $|v - v_p|$ is predominantly given by the particle velocity v, and so we have the following approximation:

$$|v - \sqrt{\epsilon}\omega| \approx \begin{cases} |v| - \sqrt{\epsilon}\omega, & v \geq 0 \\ |v| + \sqrt{\epsilon}\omega, & v < 0 \end{cases} = |v| \mp \sqrt{\epsilon}\omega \tag{5.11}$$

5.2.2. Computing integrals

The first integral we need to compute, from the term (5.9), is:

$$2\sqrt{\epsilon}\int_{-\infty}^{\infty}|v-\sqrt{\epsilon}\omega|\big[-v\omega f_\epsilon-\omega f_\epsilon'\big]\mathscr{M}\,d\omega$$

Using (5.11) we can rewrite the absolute value term. Moreover, we will make use of the fact that $v=\pm|v|$ to bring the whole expression in terms of $|v|$. Hence the integral we need to compute is:

$$2\sqrt{\epsilon}\int_{-\infty}^{\infty}(|v|\mp\sqrt{\epsilon}\omega)\big[\mp|v|\omega f_\epsilon-\omega f_\epsilon'\big]\mathscr{M}\,d\omega \tag{5.12}$$

Expanding the bracketed terms we have:

$$(5.12)=2\sqrt{\epsilon}\int_{-\infty}^{\infty}\Big(\mp|v|^2f_\epsilon\omega+\sqrt{\epsilon}|v|f_\epsilon\omega^2-|v|f_\epsilon'\omega\pm\sqrt{\epsilon}f_\epsilon\omega^2\Big)\mathscr{M}\,d\omega$$

Using the following shorthand $I_n=\int_{-\infty}^{\infty}\omega^n\mathscr{M}(\omega)\,d\omega$, we can rewrite this into the following:

$$(5.12)=\mp2\sqrt{\epsilon}|v|^2f_\epsilon I_1+2\epsilon|v|f_\epsilon I_2-2\sqrt{\epsilon}|v|f_\epsilon'I_1\pm2\epsilon f_\epsilon I_2=2\sqrt{\epsilon}\big(\mp|v|^2f_\epsilon-|v|f_\epsilon'\big)I_1+2\epsilon\big(|v|f_\epsilon\pm f_\epsilon'\big)I_2 \tag{5.13}$$

We will now proceed onto the next integral, from the term (5.10). Using the same substitutions (Eq. 5.11 and $v=\pm|v|$), we get:

$$2\epsilon\int_0^{\infty}(|v|\mp\sqrt{\epsilon}\omega)\big[|v|^2(\omega^2-1)f_\epsilon\pm2|v|\omega^2f_\epsilon'+\omega^2f_\epsilon''+\omega^2f_\epsilon\mp|v|f_\epsilon'\big]\mathscr{M}\,d\omega \tag{5.14}$$

We will discard the $\sqrt{\epsilon}\omega$ term at the start, as it gives us a total $\mathscr{O}(\epsilon^{3/2})$. Using the same notational shorthand of I_n we get:

$$(5.14)=2\epsilon\Big(|v|^3f_\epsilon(I_2-I_0)\pm2|v|^2f_\epsilon'I_2+|v|f_\epsilon''I_2+|v|f_\epsilon I_2\mp|v|^2f_\epsilon'I_0\Big)+\mathscr{O}(\epsilon^{3/2}) \tag{5.15}$$

We will now compute the simpler integrals I_0,I_1,I_2 to obtain a closed expression for (5.13) and (5.15). These are well-established results, they are namely the moments up to the second order of the standard normal distribution, hence:

$$\begin{aligned}I_0&:=\int_{-\infty}^{\infty}\mathscr{M}\,d\omega=1\\ I_1&:=\int_{-\infty}^{\infty}\omega\mathscr{M}\,d\omega=0\\ I_2&:=\int_{-\infty}^{\infty}\omega^2\mathscr{M}\,d\omega=\Big(\mathbb{V}\mathrm{ar}(\mathscr{M})-\mathbb{E}[\mathscr{M}]^2\Big)=1\end{aligned}$$

In the last integral, we note that we are computing the second moment, which can be linked to the variance and mean (as $\mathbb{V}\mathrm{ar}(X)=\mathbb{E}[X^2]-\mathbb{E}[X]^2$). Since $\mathscr{M}(\omega)$ is a standard normal distribution in ω, the mean is 0, and the variance is 1, giving the result. With these integrals evaluated, we can evaluate and combine Eqs. (5.13) and (5.15) into:

$$2\epsilon\Big(|v|f_\epsilon\pm f_\epsilon'\pm2|v|^2f_\epsilon'+|v|f_\epsilon''+|v|f_\epsilon\mp|v|^2f_\epsilon'\Big)+\mathscr{O}(\epsilon^{3/2})$$

We simplify this by noting that $\pm=\mathrm{sgn}(v)$, and $\pm|v|=v$. This gives us our final result:

$$\partial_tf_\epsilon=2\epsilon\Big(2|v|f_\epsilon+\mathrm{sgn}(v)f_\epsilon'+v|v|f_\epsilon'+|v|f_\epsilon''\Big)+\mathscr{O}(\epsilon^{3/2}) \tag{5.16}$$

5.2.3. Identifying the Fokker-Planck equation

Applying the time scaling limit (5.5), we get $\partial_t=\partial_\tau\cdot\partial_t(\tau)=2\epsilon\partial_\tau$. Hence rearranging (5.16) gives us our final equation:

$$\partial_\tau f_\epsilon=2|v|f_\epsilon+\mathrm{sgn}(v)f_\epsilon'+v|v|f_\epsilon'+|v|f_\epsilon''+\mathscr{O}(\epsilon^{1/2})$$

Taking the limit of $\epsilon\to0$, the higher order terms of ϵ will naturally go to zero. Hence:

$$\lim_{\epsilon\to0}\partial_\tau f_\epsilon=2|v|f+\mathrm{sgn}(v)f'+v|v|f'+|v|f''$$

This equation is what we desired! How so? See that we can rewrite the f'' term as the derivative of a product. We get:

$$2|v|f + \text{sgn}(v)f' + v|v|f' + |v|f'' = \partial_v(|v|f') + 2|v|f + v|v|f' = \partial_v(|v|f' + v|v|f)$$

This is exactly of the form of our desired kinetic Fokker-Planck equation (4.5), restated below:

$$\partial_t f = \nabla_v \cdot (|\vec{v}|\nabla_v f + \vec{v}|\vec{v}|f) \overset{\vec{v}\in\mathbb{R}^1}{=} \partial_v(|v|\partial_v f + v|v|f)$$

So we have successfully derived the kinetic Fokker-Planck equation as we set out to do.

5.3. Discussion

One may comment on the presence the 2 in the substitution expression for τ (5.5). This is merely a scaling constant to account for the extra 2 acquired in the derivation. One may also wonder to what extent the assumption giving rise to Eq. 5.11 actually holds, and how much of an error this approximation incurs. In any case, the validity of the assumptions are of interest, and future work may perhaps delve into the use of simulation work to validate (in particular) assumption 1 of the Maxwellian piston, for a general particle simulation on a mathematical torus near an equilibrium state (e.g. that the particle velocity distribution is Maxwellian).

6

Conclusion

In this thesis, we discussed at length the adiabatic piston paradox, the kinetic theory behind it and the simulation techniques. General results on the convergence of equilibrium provided us with a toolkit of mathematical techniques to determine the rate of convergence of a set of Fokker-Planck equations. These results have been generalized in [1, 22] for a more elaborate set of Fokker-Planck equations. Throughout our derivation process, we used the assumption of spatial homogeneity to greatly simplify our work. Introducing the spatial dimensions, the results become a lot harder to derive, as the system tends to approach a local equilibrium (for each $\vec{x}$, the velocity distribution $f(t,\vec{x},\cdot)$ converges to the entropically minimal distribution). This, however, introduces a degree of degeneracy. Fortunately, for the linear Fokker-Planck equation, one has a set of results [12], once again based on logarithmic Sobolev inequalities like that of Theorem 4.3.4.

For the adiabatic piston paradox itself, we have noted there are many different limiting schemes, involving taking the piston mass, number of molecules, and volume of the box to infinity (without diluting the dilute gas assumptions). We investigated the scaling limits of Chernov and Lebowitz's work [9, 10], and separately derived a different macroscopic equation in Chapter 5. The variety of limits and the different equations that, then, describe the piston paradox adds a level of complexity. Although it is rather well-established that the piston will move to accommodate thermal equilibrium, it is unclear if random thermal fluctuations will still cause minor fluctuations. These fluctuations would not appear in any scaling analysis where $N \to \infty$ as they get 'averaged out', but fortunately the recent work of Khalil [20] has derived a kinetic equation of motion (similar to the Boltzmann equation) for the finite case, though with still a few assumptions. Furthermore, they have managed to prove a H-theorem result, implying a generalized level of convergence.

As we have seen before, the theoretical scaling limits and subsequent equations that describe the piston motion can be investigated through computer simulations [6, 21]. We would therefore hope to use the efficient algorithm we implemented from [29] in Chapter 3 to confirm the theoretical assumptions for our derivation in Chapter 5. Indeed, the case of the adiabatic piston paradox in a mathematical torus/periodic boundary conditions leads to the additional conservation of momentum, which may lead to the piston drifting in one direction. To this end, we expect the optimization results from Figure 3.5 to be useful.

One could also use the algorithm to see what happens in the context of the scaling limits of Section 3.1.2, for different initial velocity distributions. Although this is mentioned briefly in the works of [4], that the specific distribution they chose (Eq. 3.3) leads to unstable results, one may wonder how the Maxwellian distribution would fare, and a convex combination of the two distributions. One could also investigate through means of an ensemble of simulation runs how the velocity distribution of a particle develops over time, and if it agrees with any particular derived equation.

There is also the question of the optimality of the algorithm in the context of the piston paradox. We expect that the empirical scaling relations in Figures 3.6 and 3.7 can be derived in the context of the piston paradox, and that eventually the theoretical minimum of $\mathcal{O}(N_c \log N) = \mathcal{O}(N \log N)$ can be recovered. To do so, however, one would also have to account for the influence of other parameters, such as the piston length, on the computation times. This optimal algorithmic running time relation could also be potentially recov-

ered through implementing the varying cell lengths, as discussed in Section 3.4.1.

Although the piston paradox is one that is firmly rooted in theoretical physics - no real-life piston wall could exist without permitting heat to pass through the two systems (by conduction, or friction, etc.) - research into the paradox has uncovered the intricate dance between mesoscopic and microscopic descriptions of physical systems. And from a mathematical perspective, the task of formalizing the physical intuitions and assumptions, i.e. deriving them from a generic mathematical description, is still an unfinished job.

Acknowledgements

I would like to thank both my supervisors, Dr. Havva Yoldaş and Dr. ir. Danny Lathouwers for their guidance and supervision, and in particular for their help in deriving the kinetic equation in Chapter 5.

Bibliography

[1] Giuseppe Toscani Anton Arnold, Peter Markowich and Andreas Unterreiter. On convex sobolev inequalities and the rate of convergence to equilibrium for fokker-planck type equations. *Communications in Partial Differential Equations*, 26(1-2):43–100, 2001. doi: 10.1081/PDE-100002246. URL https://doi.org/10.1081/PDE-100002246.

[2] A. A. Arsen'ev and O. E. Buryak. On the Connection Between a Solution of the Boltzmann Equation and a Solution of the Landau-Fokker Equation. *Sbornik: Mathematics*, 69(2):465–478, February 1991. doi: 10.1070/SM1991v069n02ABEH001244.

[3] L. Boltzmann. *Lectures on gas theory*. University of California Press, Berkeley, 1964. Translated by Stephen G. Brush. Reprint of the 1896-1898 edition.

[4] E Caglioti, N Chernov, and J L Lebowitz. Stability of solutions of hydrodynamic equations describing the scaling limit of a massive piston in an ideal gas. *Nonlinearity*, 17(3):897, feb 2004. doi: 10.1088/0951-7715/17/3/009. URL https://dx.doi.org/10.1088/0951-7715/17/3/009.

[5] Herbert B Callen. *Thermodynamics and an Introduction to Thermostatistics*. John Wiley & Sons, New York, 1960.

[6] Massimo Cencini, Luigi Palatella, Simone Pigolotti, and Angelo Vulpiani. Macroscopic equations for the adiabatic piston. *Physical review. E, Statistical, nonlinear, and soft matter physics*, 76:051103, 12 2007. doi: 10.1103/PhysRevE.76.051103.

[7] Carlo Cercignani, Reinhard Illner, and Mario Pulvirenti. *Informal Derivation of the Boltzmann Equation*, pages 13–32. Springer New York, New York, NY, 1994. ISBN 978-1-4419-8524-8. doi: 10.1007/978-1-4419-8524-8_3. URL https://doi.org/10.1007/978-1-4419-8524-8_3.

[8] S. Chandrasekhar. Stochastic problems in physics and astronomy. *Rev. Mod. Phys.*, 15:1–89, Jan 1943. doi: 10.1103/RevModPhys.15.1. URL https://link.aps.org/doi/10.1103/RevModPhys.15.1.

[9] N. Chernov and Joel Lebowitz. Dynamics of a massive piston in an ideal gas: Oscillatory motion and approach to equilibrium. *Journal of Statistical Physics*, 109, 06 2002. doi: 10.1023/A:1020450228657.

[10] N I Chernov, J L Lebowitz, and Yakov G Sinai. Dynamics of a massive piston in an ideal gas. *Russian Mathematical Surveys*, 57(6):1045, dec 2002. doi: 10.1070/RM2002v057n06ABEH000572. URL https://dx.doi.org/10.1070/RM2002v057n06ABEH000572.

[11] Thomas H. Cormen, Charles E. Leiserson, Ronald L. Rivest, and Clifford Stein. *Introduction to Algorithms, Third Edition*. The MIT Press, 3rd edition, 2009. ISBN 0262033844.

[12] Laurent Desvillettes and Cédric Villani. On the trend to global equilibrium in spatially inhomogeneous entropy-dissipating systems: The linear Fokker-Planck equation. *Commun. Pure Appl. Math.*, 54(1):1–42, January 2001.

[13] Aleksandar Donev, Salvatore Torquato, and Frank H. Stillinger. Neighbor list collision-driven molecular dynamics simulation for nonspherical hard particles. i. algorithmic details. *Journal of Computational Physics*, 202(2):737–764, 2005. ISSN 0021-9991. doi: https://doi.org/10.1016/j.jcp.2004.08.014. URL https://www.sciencedirect.com/science/article/pii/S0021999104003146.

[14] R.P. Feynman, R.B. Leighton, M. Sands, and EM Hafner. *The Feynman Lectures on Physics; Vol. I*, volume 33. AAPT, 1965.

[15] A. D. Fokker. Die mittlere energie rotierender elektrischer dipole im strahlungsfeld. *Annalen der Physik*, 348(5):810–820, 1914. doi: https://doi.org/10.1002/andp.19143480507. URL https://onlinelibrary.wiley.com/doi/abs/10.1002/andp.19143480507.

[16] Gustavo L. Gilardoni. On Pinsker's and Vajda's type inequalities for Csiszár's f -divergences. *IEEE Transactions on Information Theory*, 56(11):5377–5386, 2010. doi: 10.1109/TIT.2010.2068710.

[17] L. Gross. Logarithmic Sobolev inequalities. *Amer. J. Math*, 97, 1975.

[18] Alberto Herrera-Gomez. The thermodynamic equilibrium of gas in a box divided by a piston. 03 2010. URL https://arxiv.org/ftp/arxiv/papers/1003/1003.1556.pdf.

[19] E Kestemont, C. Van den Broeck, and M. Malek Mansour. The "adiabatic" piston: And yet it moves. *Europhysics Letters (EPL)*, 49(2):143–149, January 2000. ISSN 1286-4854. doi: 10.1209/epl/i2000-00129-8. URL http://dx.doi.org/10.1209/epl/i2000-00129-8.

[20] Nagi Khalil. Mesoscopic description of the adiabatic piston: Kinetic equations and $\mathscr{H}$-theorem. *Journal of Statistical Physics*, 176(5):1138–1160, June 2019. ISSN 1572-9613. doi: 10.1007/s10955-019-02336-x. URL http://dx.doi.org/10.1007/s10955-019-02336-x.

[21] M. Malek Mansour, Alejandro Garcia, and Florence Baras. Hydrodynamic description of the adiabatic piston. *Physical review. E, Statistical, nonlinear, and soft matter physics*, 73:016121, 02 2006. doi: 10.1103/PhysRevE.73.016121.

[22] Peter Markowich and Cédric Villani. On the trend to equilibrium for the fokker-planck equation: An interplay between physics and functional analysis. *Mathematica Contemporanea*, 19, 05 2000.

[23] Makoto Matsumoto and Takuji Nishimura. Mersenne twister: a 623-dimensionally equidistributed uniform pseudo-random number generator. *ACM Trans. Model. Comput. Simul.*, 8(1):3–30, jan 1998. ISSN 1049-3301. doi: 10.1145/272991.272995. URL https://doi.org/10.1145/272991.272995.

[24] J. Maxwell. On the dynamical theory of gases. *Philos. Trans. Roy. Soc. London*, 157, 1867. doi: https://doi.org/10.1098/rstl.1867.0004.

[25] Edward Nelson. *Dynamical theories of Brownian motion*. Princeton University Press, 1967.

[26] J. Piasecki and Ya. G. Sinai. *A Model of Non-Equilibrium Statistical Mechanics*, pages 191–199. Springer Netherlands, Dordrecht, 2002. ISBN 978-94-011-4365-3. doi: 10.1007/978-94-011-4365-3_10. URL https://doi.org/10.1007/978-94-011-4365-3_10.

[27] M. Planck. Über einen Satz der statistischen Dynamik und seine Erweiterung in der Quantentheorie, 1917. URL https://biodiversitylibrary.org/page/29213319. Sitzungsberichte der Preussischen Akademie der Wissenschaften zu Berlin. 24:324–341.

[28] Grant Rydquist and Mahdi Esmaily. An optimal o(n) scheme for simulations of colliding, particle-laden flows on unstructured grids. *Journal of Computational Physics*, 420:109703, 2020. ISSN 0021-9991. doi: https://doi.org/10.1016/j.jcp.2020.109703. URL https://www.sciencedirect.com/science/article/pii/S0021999120304770.

[29] Hersir Sigurgeirsson, Andrew Stuart, and Wing-Lok Wan. Algorithms for particle-field simulations with collisions. *Journal of Computational Physics*, 172(2):766–807, 2001. ISSN 0021-9991. doi: https://doi.org/10.1006/jcph.2001.6858. URL https://www.sciencedirect.com/science/article/pii/S0021999101968585.

[30] Cédric Villani. A review of mathematical topics in collisional kinetic theory. *Handbook of Mathematical Fluid Dynamics*, 1, 12 2002. doi: 10.1016/S1874-5792(02)80004-0.